Thesis for the degree
Doctor of Philosophy

Submitted to the Scientific Council of the
Weizmann Institute of Science
Rehovot, Israel

עבודת גמר (תזה) לתואר
דוקטור לפילוסופיה

מוגשת למועצה המדעית של
מכון ויצמן למדע
רחובות, ישראל

במתכונת "רגילה"
In a "Regular" Format

By
Diana Varol

מאת
דיאנה ורול

הבנת מעורבות האנזים דייסר ומולקולות המיקרו רנ״א בתפקוד תאי המיקרוגליה במערכת העצבים, בזמן ההתפתחות העוברית ובעכבר הבוגר

Studying the role of dicer and microRNAs in microglia of the developing and adult brain

Advisor:
Prof. Steffen Jung

מנחה:
פרופ' סטפן יונג

November 2014

חשוון, תשע"ה

Acknowledgment

I would like to express my sincere gratitude to my supervisor and mentor Prof. Steffen Jung for the opportunities, guidance and support during my graduate studies in his laboratory. Especially, I would like to thank him for sharing with me his knowledge, enthusiasm, curiosity, and devotion to science.

I would like to thank the members of the Jung laboratory for their support, assistance and friendship during these years.

I would like to express my gratitude to our collaborator, Prof. Marco Printz from the Universitats Klinikum, Freiburg, Germany for his kind consultation and assistance in the performance of the histological analysis of microgila phenotype and activity.

Last but not least I would like to thank my amazing parents and husband for their support and help along this period, and to my baby girl Tamar for being the sunshine of my life.

Table of contents

1. Introduction 9

1.1 Microglia are the resident macrophages of the CNS. 9

1.2 Microglia regulate neuronal wiring in the developing and adult CNS. 10

1.2.1 Microglia are involved in embryonic development. 10

1.2.2 Microglia are involved in post-natal development. 11

1.2.3 Adult and embryonic microglia differ in phenotype. 13

1.3 Microglia function during pathology. 14

1.4 MicroRNAs (MiRs) regulate homeostatic and pathologic processes in the CNS. 16

1.4.1 MiR generation is dependent on *Dicer*. 16

1.4.2 MiRs regulate neurodegenerative diseases. 17

1.4.3 MiRs regulate microglia phenotype and function. 18

1.5 Genetic manipulation of microglia in context -- *Cx3cr1*^{Cre} and *Cx3cr1*^{CreER} mice. 20

2. Results

2.1 Microglia display a unique transcriptome and microRNA profile distinct from other tissue resident macrophages. 21

2.2 Establishment of mice harboring a constitutive Dicer-deficiency in microglia. 23

2.3 *Cx3cr1*^{Cre}*:Dicer*$^{fl/fl}$ mice display a reduced motoric function. 24

2.4 Microglial *Dicer* deficiency results in astrocytosis at specific brain areas related to motoric activity. 26

2.5 *Cx3cr1*^{Cre}*:Dicer*$^{fl/fl}$ mice display astrocytosis, and reduced motor neuron numbers in the L5 ventral horn of the spinal cord. 28

2.6 *Cx3cr1*^{Cre}*:Dicer*$^{fl/fl}$ mice show an accumulation of Mac2^{+} phagocytic cells and a reduced number of axons in L5- ventral root. 31

2.7 Histological evaluation of *Cx3cr1*^{Cre}*:Dicer*$^{fl/fl}$ microglia reveals their activation and increased turnover. 32

2.7.1 Dicer-deficient microglia show an activated phenotype. 32

2.7.2 Dicer-deficient microglia display increased cell proliferation and apoptosis. 36

2.8 Microarray analysis of the mRNA of *Dicer*-deficient microglia reveals their activation and loss of unique homeostatic gene signature. 38
2.9 Reconstitution of *Dicer*-deficient microglia by BM-derived WT brain macrophages does not rescue the motoric-deficiency. 41
2.10 *Cx3cr1*^{Cre}*:Dicer*$^{fl/fl}$ mice show a depletion of skin resident cells including Langerhans cells (LC) and dendritic epidermal T cells (DETCs). 45
2.11 Post-natal induction of *Dicer* loss in microglia, utilizing *Cx3cr1*$^{\underline{CreER}}$*:Dicer*$^{fl/-}$ mouse model. 46
2.11.1 *Cx3cr1*^{CreER}*:Dicer*$^{fl/-}$ *mice show an efficient Dicer loss in microglia.* 46
2.11.2 Unchallenged *Cx3cr1*^{CreER}*:Dicer*$^{fl/-}$ mice display no overt phenotype. 47
2.11.3 Microglia of *Cx3cr1*^{CreER}*:Dicer*$^{fl/-}$ mice are radio-sensitive. 49
3. Materials and Methods. 51
4. Discussion 56
5. Declaration 62
6. References 63

List of abbreviations

AD	Alzheimer's Disease
ALS	Amyotrophic Lateral Sclerosis
BBB	Brain Blood Barrier
CNS	Central Nervous System
DAMP	Death Associated Molecular Patterns
EAE	Experimental Autoimmune Encephalitis
FACS	Flourescent Activated Cell Sorting
GFP	Green Fluorescent Proein
Il6	Ilnterleukin 6
iNOS	inducible Nitric Oxide Synthase
i.v	*Intravenously*
LC	Langehans cells
L5	Lumbar 5
miR	micro-RNA
MMP	Matrix Metallo Proteinase
mSOD1	mutant Cu/Zn Super Oxide Dismutase
MS	Multiple Sclerosis
NO	Nitric Oxide
Nox2	NADPH oxidase 2
NFkB	Nuclear Factor Kappa B
PAMP	Pathogen Associated Molecular Patterns
PD	Parkinson’s disease
PFA	Para-Form-Aldhyde
PNS	Peripheral Nervous System
PRR	Pattern Recognition receptor
SC	Spinal chord
TAM	Tamoxifen
TAK1	TGFβ activated kinase1
TGFβ	Transforming Growth Factor β
TLR	Toll Like Receptors
TNF	Tumor Necrosis Factor
YFP	Yellow Flourescent Protein

Abstract

Microglia are the resident macrophage population of the central nervous system (CNS), arising early during development from CX_3CR1^+ progenitors in the embryonic yolk sac and, remarkably, persisting throughout life. Microglia function as immune sentinels to cope with infection or tissue damage, but these cells are also involved in the establishment and maintenance of neuronal circuits, regulating neurogenesis, neuronal differentiation and synaptic remodeling. To protect the CNS from harmful inflammation, the microglia activity is believed to be tightly regulated by various factors including microRNAs (miRs). Inadequate miR regulation is an emerging mechanism involved in various neurodegenerative disorders, as demonstrated by the respective small animal models. Here, we generated a conditional miR deficiency in microglia by crossing *Cx3cr1*^{Cre} and *Cx3cr1*^{CreER} mice with mice harboring a conditional allele of *Dicer*, the main miR-processing enzyme. In *Cx3cr1*^{Cre}*:Dicer*$^{fl/fl}$ animals, microglia are targeted during embryonic development, while *Cx3cr1*^{CreER}*:Dicer*$^{fl/-}$ microglia were targeted postnataly, upon tamoxifen administration. Strikingly, a microglial *Dicer* deficiency introduced during embryonic development, but not at adulthood resulted in strong microglia activation, as well as the development of motoric impairment of the hind limbs. In contrast, the introduction of the microglial *Dicer* deficiency in adult microglia did not yield any overt phenotype in unchallenged animals. Interestingly though, the *Dicer* deficiency turned the otherwise radio-resistant adult microglia into radio-sensitive. Collectively, our results highlight the importance of miRs in microglia-dependent establishment and maintenance of neuronal networks during embryonic development, but suggest that adult microglial homeostasis is uniquely robust in that it can be maintained in absence of post-transcriptional control by miRs.

<u>תקציר</u>

מיקרוגליה הם המקרופאג'ים המקומיים של מערכת העצבים המרכזית, הנוצרים בשלב מוקדם של ההתפתחות העוברית מתאי קדמון המגיעים משק החלמון העוברי ומאופיינים ע"י ביטוי של הקולטן לכמוקין פרקטלקיין (CX_3CR1). באופן מופלא, המיקרוגליה שנוצרים בזמן ההתפתחות העוברית שורדים לאורך תוחלת החיים. מיקרוגליה מתפרדים כתאים שומרים של מערכת החיסון ומעורבים בהתפתחות ותחזוקה של מעגלים של תאי עצב ומעגלים עצביים, ההתמיינות של תאי עצב ועיצוב של הסינפסות העצביות. בכדי להגן על מערכת העצבים המרכזית מנזק דלקתי, הפעילות של תאי המיקרוגליה מבוקרת בקפדנות ע"י פקטורים שונים ובינהם מיקרו RNA (miRs). מממצאים שנאספו בעבודות קודמות המבוססות על מודלים בחיות מעבדה עולה ההשערה שבקרה לא תקינה של miRs מהווה חלק מהמנגנון גורם המחלה במגוון מחלות ניוון עצבי. בעבודת התיזה הנוכחית, יצרנו מודל חדשני ובו אנחנו משרים חסר של miRs ספציפית בתאי מיקרוגליה ע"י הכלאה בין עכברים מסוג *$Cx3cr1^{Cre}$* ו *$Cx3cr1^{CreER}$* עם עכברים שמכילים חסר מותנה של הגן המקודד ל Dicer (*$Dicer^{fl/fl}$*), שהינו האנזים העיקרי האחראי על ייצור ועיבוד של miRs. חשוב לציין שבעכברי *$Cx3cr1^{Cre}$:$Dicer^{fl/fl}$* (Cre-*Dicer*) המיקרוגליה יבטאו את החסר ל Dicer בזמן ההתפתחות העוברית, בעוד שבעכברי *$Cx3cr1^{CreER}$:$Dicer^{fl/fl}$* חסר זה מושרה בתאים אלו לאחר הלידה ע"י טיפול בטמוקסיפן (Tamoxifen). באופן ניכר, חסר בגן זה בזמן ההתפתחות העוברית גרם לשפעול ניכר של תאי המיקרוגליה ולהתפתחות של ליקוי תנועתי של הרגלים האחוריות. בניגוד, השרייה של חסר בגן זה במיקרוגליה בזמן בגרות לא גרם לאיזשהו פנוטיפ גלוי בחיות לא מאותגרות. יחד עם זאת, בשני המקרים החסר ב *Dicer* הפך את תאי המיקרוגליה, שהינם בד"כ עמידים לקרינה, לרגישים לקרינה. לסיכום, התוצאות שלנו מדגישות את החשיבות של miRs בבקרה של יצירת ותחזוקת רשתות עצביות בזמן ההתפתחות העוברית, אך גם מרמזות שהפעילות של תאי המיקרוגליה הבוגרים בזמן שיגרה נתונה לבקרה אדוקה, אך שאינה תלויה ב miRs.

1. Introduction

1.1. Microglia are the resident macrophages of the CNS.

Microglia are hematopoietic cells that develop independently of neuroectoderm-derived neurons, astrocytes and oligodendrocytes. They are members of the mononuclear phagocyte system (MPS) alongside other macrophages monocytes and dendritic cells [1]. Sequestered behind the blood brain barrier (BBB) in the unique neuronal/microglial context, microglia display a gene expression profile that significantly differs from other tissue macrophages [2]. The microglia compartment is established before birth from an early "primitive" hematopoietic wave originating from CX_3CR1^+ yolk sac macrophages populating the CNS as early as embryonic day 9.5 (E 9.5) [3] (**Scheme 1**). The mature microglia pool subsequently maintains itself throughout adulthood due to longevity and limited self-renewal [4]. Microglia share this prenatal ontogeny with other resident tissue macrophage populations [1], however the latter seem less secluded and more promiscuous with respect to the incorporation of monocytic cells derived from the fetal liver during embryonic development, as well as monocytes derived from the bone-marrow (BM) during challenge [5]. Nevertheless, BM derived monocytes were also shown to populate the injured central nervous system (CNS) giving rise to a macrophage-type of cells [3] **(Scheme 1).** Depending on the time and route of their arrival to the tissue and on the local milieu, they contribute to both pro- and anti-inflammatory activities [5, 6]. However, these cells do not seem to permanently seed the CNS; rather, an homeostatic state relying solely on microglia seems to be restored after inflammation is resolved [5].

Steady state microglia, that are present throughout the normal adult CNS parenchyma, actively sample their surroundings by extending and retracting processes [7, 8]. They were shown to play pivotal homeostatic roles during development and adulthood, related to synaptic remodeling and phagocytosis of dying neurons [9-11]. During neurodegenerative disease, however, microglia become activated and acquire a distinct phenotype with pleiotropic functions [12], mostly harmful, depending on disease model and stage. Little is known about molecular patterns controlling the microglia phenotype in homeostasis and disease. In addition, due to lack of experimental systems allowing targeted manipulation of microglia *in vivo*, much of our knowledge about the function of microglia is obtained from *in vitro* culture studies.

Under these conditions, microglia were shown to loose much of their uniqueness and turn into prototype macrophages [13].

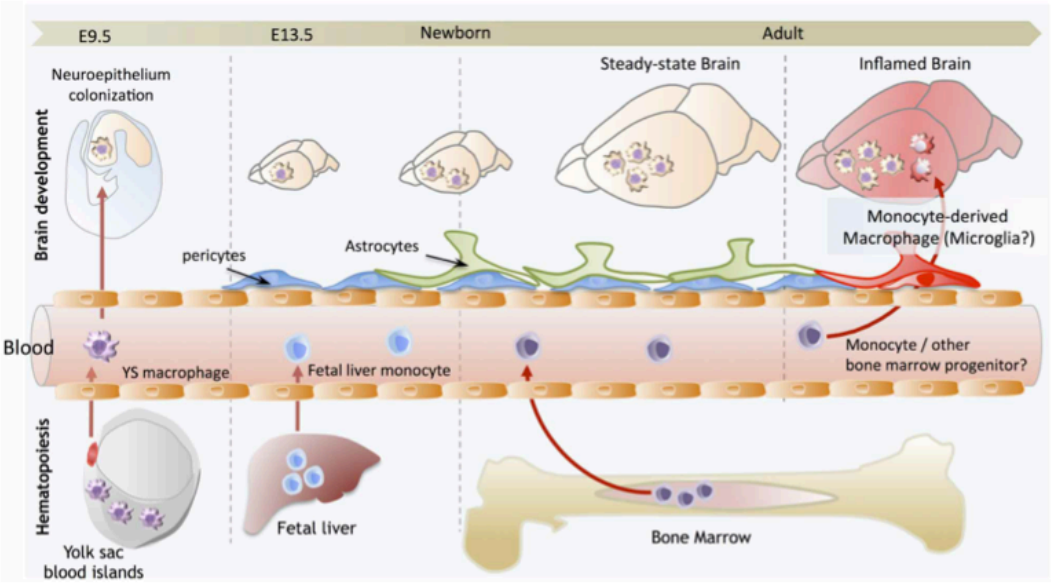

Scheme 1: Microglia precursors populate the brain during embryonic development. Primitive macrophages exit the yolk sac blood islands at the onset of circulation and colonize the neuroepithelium from E9.5 to establish the microglia population. The blood brain barrier starts to form from E9.5 and may isolate the developing brain from the contribution of fetal liver hematopoiesis. Embryonic microglia expand and colonize the whole CNS until adulthood. Importantly, in steady state conditions, embryo-derived microglia maintain themselves with limited self-renewal and are not dependent on blood-derived cells for their replenishment. Nevertheless, during certain inflammatory conditions, the recruitment of monocytes or other bone marrow-derived progenitors can supplement the microglial population to some extent, but they are eventually cleared from the CNS environment [14]. [3]

1.2. Microglia regulate neuronal wiring in the developing and adult CNS.

As the principal CNS immune cells, microglia represent the first line of defense in response to exogenous threats. Past studies have largely been dedicated to defining the complex immune functions of microglia. However, novel insights about microglia involvement in neuronal wiring have accumulated recently. It is now clear that microglia are critically involved in shaping neural circuits pre-natally [15, 16], in early life [9, 10, 17] and adulthood [18-20].

1.2.1 Microglia are involved in embryonic development.

Microglia are the first glial cells appearing in the CNS [4, 21], prior to astrocytes and oligodendrocytes, suggesting the existence of exclusive microglia-neuron interactions. This early brain colonization by microglia is a highly conserved feature across vertebrate species [22-26]. Embryonic neural development involves

programmed cell death of various neuronal sub-types [27, 28], and microglia are critical for the phagocytosis and removal of these dying neurons in order to prevent tissue damage [15, 27, 29]. In addition to their role in clearing debris, microglia are considered critical players in brain development and neural circuitry formation [30, 31]. They are associated with brain vascularization, neuronal proliferation, and neural cell differentiation to a neuronal or astrocyte lineage [32-34]. Examples for neuronal fate regulation are shown by the ability of microglia to facilitate neurogenesis of embryonic cortical cells [35], and differentiation of basal forebrain progenitors into cholinergic neurons [36]. In addition, microglia were shown to act on neuronal connectivity via processes termed synaptic pruning and axonal guidance. The later was displayed by their ability to attenuate dopaminergic axon outgrowth in the striatum, suggesting microglia deficiencies might cause abnormal forebrain wiring. Interestingly, this regulatory function of microglia was dependent on CX_3CR1 expression [16]. Synaptic pruning is a process of neuronal circuit fine-tuning in which microglia dependent phagocytosis is used to eliminate non-active, excess synapses generated earlier in development [9, 10, 18]. Synaptic pruning was so far documented in post-natal period and will be further described in the next section (**section 1.2.2**).

1.2.2 Microglia are involved in post-natal development.

Mouse CNS development persists in the postnatal period, including areas with on-going neurogenesis even in the adult mouse, such as the dentate gyrus (DG) of the hippocampus and the sub-ventricular zone (SVZ). Phagocytosis of dying neurons in those regions was shown to be efficiently performed by adult microglia [37]. Early life (Postnatal day 5, (P5)) microglia displayed neurotrophic functions, promoting layer 5 cortical neurons survival [17]. This activity was dependent on the expression of the chemokine receptor CX3CR1.

An intensively studied role of microglia during early life and adulthood is synaptic pruning (**Scheme 2**), involving the phagocytosis dependent elimination of access non-active synapses. Microglia dependent synaptic pruning was documented in the hippocampus, where CX_3CR1 deficient mice had immature synaptic connections [9]. In addition, microglia depletion as well as microglia-restricted BDNF deficiency caused reduction in motor-learning ability and reduced synaptic plasticity of layer V pyramidal neurons in the motor cortex [18]. Another example for experience

dependent synaptic pruning exists in the retinogeniculate system, responsible for visual input processing. Here, microglia were shown to engulf presynaptic retinal inputs projecting to the thalamus. This engulfment was mediated by complement receptor 3 (CR3) expressed on microglia recognizing complement component 3 (C3) tagging of access synapses. CR3 null mice had deficits in synaptic connectivity of this brain circuit [10].

Collectively, embryonic and adult microglia support neuronal circuit generation and remodeling, with unique functions required for each stage. Phagocytic and neurotrophic contributions of microglia can be expected to be more substantial in embryonic development, while synaptic pruning will be more pronounced in early life (sensory circuits) and to a lesser extent in the adult (learning & memory).

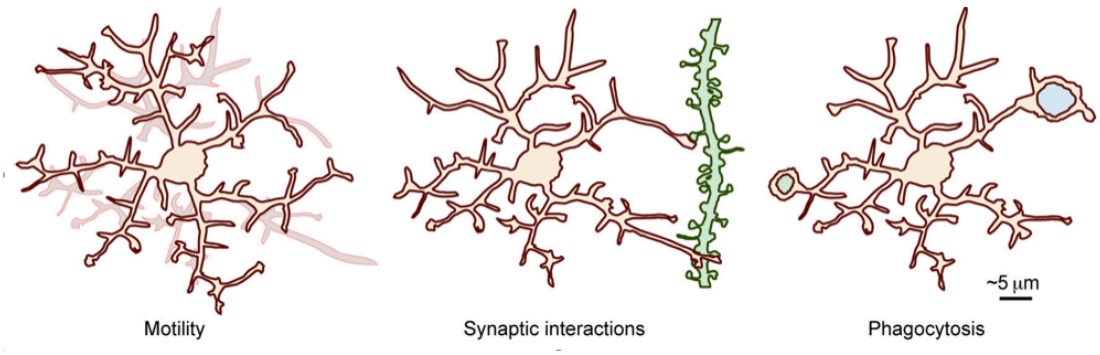

Scheme 2: Overview of microglia behavior in the healthy brain. Highly motile microglia processes continuously remodel their local environment (left), structurally and functionally interact with synaptic elements (middle; dendritic branch and spines, green) through direct contacts and exchanges of molecular signals, and contribute to restructuring of neuronal circuits by phagocytizing synaptic elements and newborn cells (right; cellular inclusions, blue and green). Microglia morphology and behavior display variability across CNS regions and stages of the lifespan. (Adopted from [38])

1.2.3 Adult and embryonic microglia differ in phenotype.

Microglia precursors originating from the yolk sac, were shown to enter the brain as early as E9.5 [4]. As opposed to adult $CD45^{lo}$ CX_3CR1^+ $F4/80^+$ $Iba1^+$ microglia, embryonic microglia display is $CD34^+CD45^{lo}CX_3CR1^+F4/80^+Iba1^+$. Furthermore, they are highly proliferative and remain as such throughout the embryonic period (**Scheme 3**) [39]. In addition, microglia have a higher migratory ability and an amoeboid morphology characterizing activated microglia [40, 41]. By P15, microglia are uniformly spread throughout the brain parenchyma and dramatically reduce their proliferative activity (**scheme 3**). This transition stage was shown to be mediated by

expression of runt related transcription factor 1 (Runx1) [42]. Adult microglia harbor a ramified shape, characterized by small cell body size and long dendrites performing continues surveillance of the surrounding parenchyma [7, 8]. They are probably actively kept in a non-inflammatory state in order to protect the delicate CNS environment. This phenotype is believed to be dictated by the local microenvironment of neurons and glia cells. Examples for neuronal molecules promoting quiescence are CD47 & CD200, interacting with CD172a/Sirpα & CD200R on microglia, respectively [43].

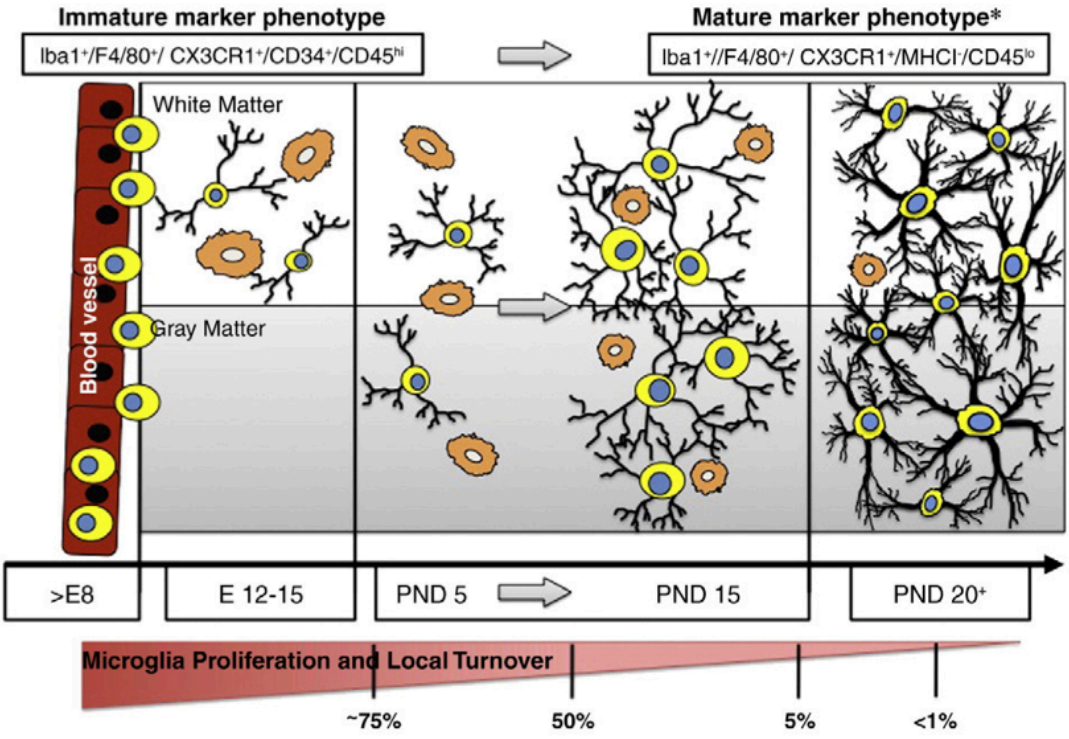

Scheme 3: Embryonic microglia are highly proliferative giving rise to the non-cycling fully differentiated adult microglia pool. During gestation (E9) microglial precursors cross the blood vessel wall and begin to take up residence in the brain parenchyma. At early stages of colonization (approx. E12–15), these cells are located in white matter regions (or along vascular/ventricular margins) possessing an amoeboid morphology similar to activated microglia (larger ruffled round cells (**orange**)). During early postnatal stages (~P5), microglia are observed in both white and gray matter regions of the brain possessing both amoeboid and process-bearing phenotypes. Between P2 to P14, microglia expand dramatically, In parallel, they also increase ratio of ramified versus amoeboid shape, with the cells having noticeably more complex process arbors and cytoplasmic material. By ~P15 microglia are well distributed throughout the brain, facilitating surveillance of the majority of the parenchyma (Adopted from [39]).

A recent study exploring the expression profile of microglia, demonstrated that adult microglia have a unique expression pattern compared with monocytes and

peripheral tissue macrophages [13] (**Scheme 4).** Interestingly, this genetic signature was highly dependent on TGFβ expression. Further comparison was performed between different stages of microglia development (Embryonic day 10 (E10), E12.5, P4, P21, P30, and adult (2 months)), revealing that genes highly expressed by adult microglia were not shared by embryonic microglia [13].

Taken together, these studies demonstrate genetic and functional differences between embryonic and adult microglia that might underlie the different requirements of the developing vs. adult neuronal environment maintained by microglia.

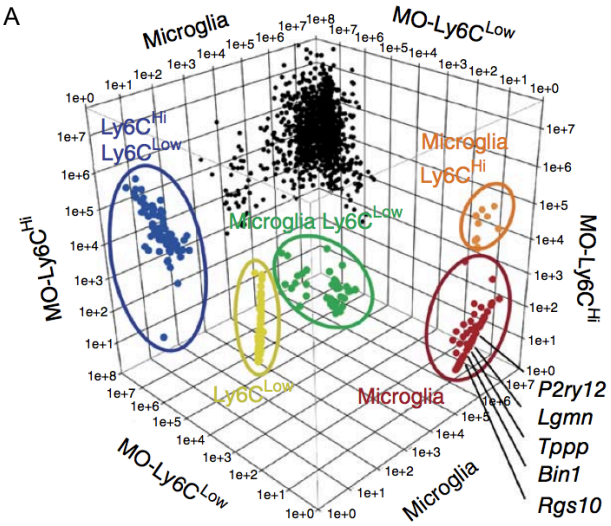

Scheme 4: Adult microglia aquire a unique expression signature. A PCA analysis of mRNA expression showing adult microglia highly express a unique set of genes (signature) differing them from monocytes and other tissue resident macrophages. (Adopted scheme from [13])

1.3 Microglia function during pathology.

Following injury or under neurodegenerative disease such as multiple sclerosis (MS), Alzheimer's disease (AD), Parkinson's disease (PD), Huntington's disease (HD), and amyotrophic lateral sclerosis (ALS), adult parenchymal microglia transform into a proliferative and motile amoeboid state in which they synthesize a large repertoire of cytokines and chemokines, produce reactive oxygen species (ROS) and exhibit increased phagocytotic activity [12, 44, 45]. Akin to other resident tissue macrophages, microglia are the primary immune sentinels of the CNS and can be activated in response to a variety of pathogen-associated molecular patterns (PAMPs) or death-associated molecular patterns (DAMPs), both recognized via pattern recognition receptors (PRR) (**Scheme 5**) [46].

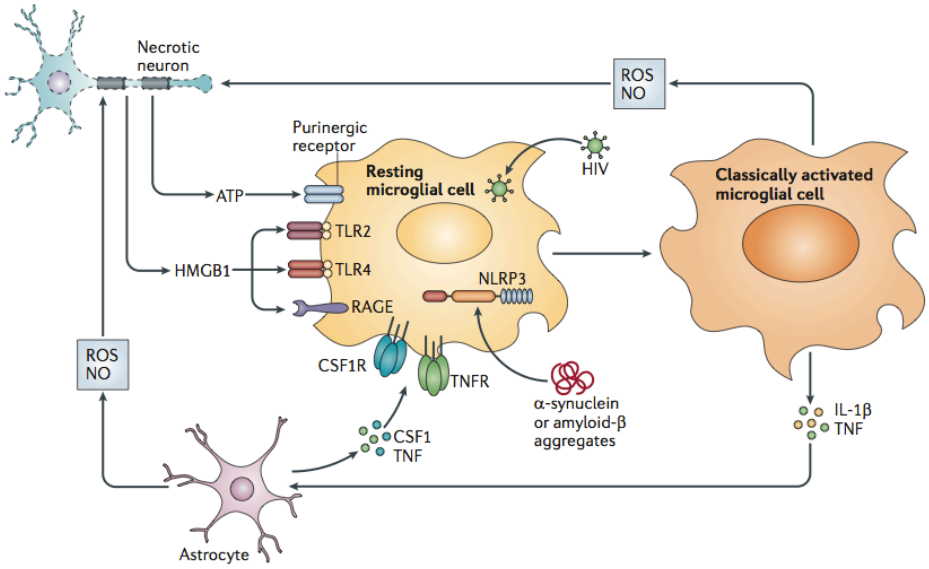

Scheme 5: Activated microglia in neurodegenerative disease. Various disease-associated factors can stimulate microglia activation via binding to PRR. Such factors include DAMPs such as high-mobility group box 1 protein (HMGB1), histones and ATP, as well as neurodegenerative disease-specific protein aggregates, such as α-synuclein or amyloid-β aggregates. Classically activated microglia also promote astrocyte activation further increasing pro-inflammatory and neurotoxic factors, which exacerbate neurodegeneration. (Adopted from [47]).

ALS is a neurodegenerative disease characterized by a progressive loss of motor neurons, leading to paralysis and death. Mutant Cu/Zn superoxide dismutase (mSOD1) is the cause for 20% of familial ALS. Transgenic mice overexpressing human mSOD1 (mSOD1 mice) develop a progressive motor neuron disease that resembles the clinical features of human familial ALS [48]. Several studies have attempted to differentiate the contribution of microglial mSOD1 mutation to disease onset and progress. One study utilized *mSOD1:PU.1*$^{-/-}$ double transgenic mice. The PU.1-deficiency causes severe lack of lymphoid and myeloid cells, including microglia. Transfer of WT, but not mSOD1, bone marrow (BM) at birth improved survival of these animals and reconstituted the microglia pool resulting in reduced motor neuron loss and slower disease progress [49]. Recently, it was shown that NFκB signaling in mononuclear phagocytes, using *Csf1r*^{Cre}: *P65*$^{fl/fl}$ mice, contributed to neuronal death in mSOD1 mice [50]. Finally, Expression profiling of mouse mSOD1 spinal chord (SC)-microglia isolated at different disease stages, revealed a significant concurrent induction of potentially neuroprotective (IGF1, osteopontin), and neurotoxic (Nox2) factors [12]

An additional neurodegenerative disease shown to critically involve an inflammatory microglia response is experimental autoimmune encephalitis (EAE), the

mouse model for MS. This model involves active immunization of mice with myelin peptide (MOG 35-55) [51]. Following immunization, SC microglia alter their phenotype from a quiescent $CD45^{int}$ MHC^{II-} mode to an active $CD45^{hi}$ $MHCII^{+}$ state [52]. We recently showed that mice lacking TGFb activated kinase1 (TAK1) exclusively in micrglia were resistant to active immunization, which resulted in a considerably less severe disease. TAK1 is considered as critical regulator of stress responses, immunity and inflammation that is mainly mediated by the downstream pathways p38MAPKK, JNK, and NF-kBp65 which are part of the microglia activation mechanism [53]. Collectively, these The above studies imply pivotal deleterious involvement of microglia in the pathophysiology of neurodegenerative disease.

1.4 MicroRNAs (MiRs) regulate homeostatic and pathologic processes in the CNS.

1.4.1 MiR generation is dependent on *Dicer*.

MiRs are a class of small (~22 nt) noncoding RNAs that negatively regulate gene-expression at the posttranscriptional level by binding to the 3′-untranslated region of target mRNAs leading to their translational inhibition or degradation [54]. A growing body of evidence suggests that miRs are important regulators of diverse biological processes such as cell differentiation, growth, proliferation, and apoptosis. Moreover, miRs are key modulators of both CNS development and plasticity [55-57]. Some miRs have been implicated in several neurological disorders, such as traumatic CNS injuries and neurodegenerative diseases [58-60]. miRs are transcribed in most cases by RNA polymerase II to primary precursor transcripts (pri-miRs) that are then processed in the nucleus by Drosha and its cofactor DiGeorge syndrome critical region gene 8 (DGCR8) into pre-miRs. The pre-miRs are transported into the cytoplasm, where *Dicer*, an RNase III-like endonuclease, further cleaves them in order to yield the mature miR (**Scheme 6**). Mature miRs bind to 3′ UTR region of their target mRNAs, inducing the posttranscriptional gene silencing mainly through mRNA destabilization [54]. A single miR can pair with the 3′UTR of hundreds of mRNAs [61]. Adding a level of complexity, miRs are also found to recognize seedless sites, 5′UTRs, and coding regions of mRNAs [62-64]. Moreover, there are a few reported cases of miRs that can activate translation of target mRNAs [65, 66].

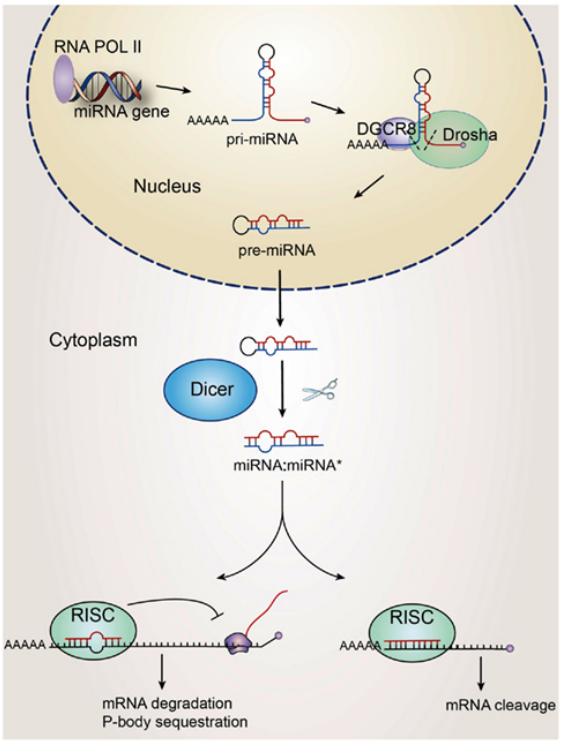

Scheme 6: Generation and function of miRs.
miRs are transcribed by RNA polymerase II as pri-miRs, which are then processed by Drosha to produce long miR precursor (pre-miR). The pre-miRs are transported to the cytoplasm where they are further cleaved by the endoribonuclease *Dicer* to mature ~22 nt long miR–miR *duplex. In this process *Dicer* interacts with the RISC complex. Within this complex, one strand of the miR duplex is removed and the single stranded miR, complementary to the target mRNA, remains in the complex and becomes functional. Seven to eight bases of the 5′ miRs "seed" sequence are partially complementary to the 3' UTR of mRNA targets, and induce posttranscriptional silencing through mechanisms such as mRNA destabilization and translational repression. Adopted from [67].

1.4.2 MiRs regulate neurodegenerative diseases.

Targeted deletion of the *Dicer* gene in selected neuronal populations results in a progressive neuronal loss associated with behavioral deficits reflecting the cell types that were targeted by the Cre-LoxP system. For example, mice lacking *Dicer* specifically in dopaminergic neurons are born alive, but develop a progressive neurodegenerative disorder manifested by 90% loss of these neurons and a resulting reduced locomotion, which is reminiscent of the phenotype of PD [68]. Conditional deletion of *Dicer* has also been used to model spinal muscular atrophy. Accordingly, by crossing between $Vacht^{Cre}$ and $Dicer^{fl/fl}$ mice, *Dicer*-deficiency is targeted into postmitotic spinal motor neurons as early as postnatal day 7 [59]. At adulthood, these mice display a phenotype characterized with astrocytosis and reduction in number of motor neurons at the Lumbar 5 (L5)-SC ventral horns, as well as hindlimb reduction of neuro-mascular junction (NMJs), pointing to a progressive neuro-degenerating disease.

Taken together, these studies demonstrate the significance of miRs in neuronal maintenance and survival, and suggest that failure of miR function could contribute to a neurodegenerative phenotype in humans. Remaining questions are which miRs are impaired functionally in specific disease states and what are the roles of individual miRs, as well as networks of miRs in these diseases. MiR206 was elevated in muscles of mSOD1 mice. Moreover, miR-206 was found required for efficient regeneration of neuromuscular junctions after nerve injury in normal mice, implying that miR-206 has beneficial effects in the mouse ALS model [69].

1.4.3 MiRs regulate microglia phenotype and function.

MiRs were shown to be involved in microglia differentiation, but also in regulating the quiescence of these cells versus their activation [70]. Deregulation of the latter could have a detrimental effect on CNS integrity. Below are several examples of specific miRs that affect microglia phenotype and function.

miR-155 promotes inflammatory response in microglia.

MiR155, broadly considered a pro-inflammatory miR, was one of the first miRs to be directly linked to a pro inflammatory phenotype [71]. MiR155 is upregulated in a microglia cell line (N9), as well as primary microglia cultures in response to LPS [72]. Moreover, miR155 induces the downregulation of the anti-inflammatory transcription factor suppressor of cytokine signaling 1 (SOCS-1) leading to the upregulation of pro-inflammatory mediators, such as iNOS, IL6, and TNFα [72]. Further supporting its pro-inflammatory role, miR-155 deficiency reduced the expression of pro-inflammatory genes in mSOD1 microglia, and resulted in an overall delay in disease progress and in extended survival [73].

MiRs -146a, -181c, and -21 down regulate inflammatory response and neurotoxicity of microglia.

MiR-146a can directly down regulate the production of pro-inflammatory cytokines by acting as a negative-feedback effector of the inflammatory signaling pathway initiated by NF-κB [71, 74]. MiR146a is significantly increased in mSOD1 microglia isolated from endstage of disease [58] however, its role in mediating microglia function during various stages of this disease model is not known. Microglia cell lines treated with anti-miR146, increased IL6 secretion following stimulation with TLR2 and 4 ligands [75]. MiR21 and miR181 are reduced in microglia activated by

hypoxia, a stroke like condition. MiR21 reduction induces FasL [76], while reduction in miR181 increases the secretion of TNFα and nitric oxide (NO), both contributing to neuronal apoptosis in culture [77].

Thus, the above studies mark miR-146a, miR181c and miR21 as negative immune-regulators of microglia pro-inflammatory response and neurotoxicity.

TGFβ induced miRs: miRs-99a, -125b, and -342-3p possibly regulate microglia homeostatic functions.

Adult microglia were shown to have a unique expression profile *in vivo,* dependent on TGFβ signaling [13]. TGFβ treatment of cultured microglia, induced a unique microglia signature, including expression of specific miRs, such as miR-99a, miR-125b-5p, and miR-342-3p, which were also enriched in freshly isolated microglia compared with other tissue resident macrophages. These miRs might constitute master regulators of the homeostatic microglia expression profile dictated by TGFβ.

Taken together, various miRs were shown to regulate microglia homeostasis and/or disease-related activation. Although of interest, much of the research about the cell biology of microglia relies currently on studies performed *in vitro*. However, cultured microglia likely were shown to loose much of their uniqueness and turn into prototype macrophages [13, 78]. Thus, the establishment of *in* vivo systems allowing the targeted genetic manipulation of miRs in microglia within their native microenvironment is critical for the elucidation of the regulatory mechanisms they govern in health and disease.

1.5 Genetic manipulation of microglia in context -- *Cx3cr1*^{Cre} and *Cx3cr1*^{CreER} mice.

The Jung laboratory has recently developed an experimental system that allows the study of microglia within their unique physiological CNS environment. Specifically, we exploited the unique high expression of the chemokine receptor CX3CR1 for the genetic manipulation of microglia [79]. *Cx3cr1*^{Cre} and *Cx3cr1*^{CreER} mice [80] were generated by targeted insertion of the respective Cre recombinase genes into the *Cx3cr1* loci, mimicking the situation of the *Cx3cr1*^{GFP} locus, previously shown to tightly reflect endogenous CX3CR1 expression [81] (**Scheme 7**). *Cx3cr1*^{Cre} mice express constitutively active Cre recombinase resulting in the spontaneous irreversible rearrangement of loxP site-flanked alleles in CX3CR1-expressing cells. In

contrast, the *Cx3cr1*^{CreER} system comprises a conditional active Cre recombinase that is fused to a mutated ligand-binding domain of the human estrogen receptor (ER) [82]. Two point mutations in the ER-LBD prevent constitutive activation of the CreER protein by endogenous estradiol, still allowing binding of the synthetic estrogen antagonist tamoxifen (TAM). In the unbound form, the CreER fusion protein resides in the cytoplasm in an inactive complex with heat shock proteins. TAM administration frees the CreER to translocate to the nucleus and mediate the site- specific recombination.

Importantly, *Cx3cr1*^{Cre} and *Cx3cr1*^{CreER} mice differ considerably with respect to the cells targeted. In *Cx3cr1*^{CreER} mice only cells that express CX3CR1 at the time of the TAM treatment are hit and will hence undergo rearrangement. In contrast, and as best demonstrated in combination with respective reporter mouse strains [80], in *Cx3cr1*^{Cre} mice also cells that are derived from CX3CR1^{+} cells but subsequently silenced CX3CR1 expression will have recombined loxP-flanked loci. *Cx3cr1*^{Cre} mice, therefore, report on the history of the cell and can be used for fate mapping. Thus, *Cx3cr1*^{Cre} will target both resident microglia and peripheral/CNS-infiltrating macrophages, whereas TAM-treated *Cx3cr1*^{CreER} mice can be used to manipulate microglia only (**Scheme 7**).

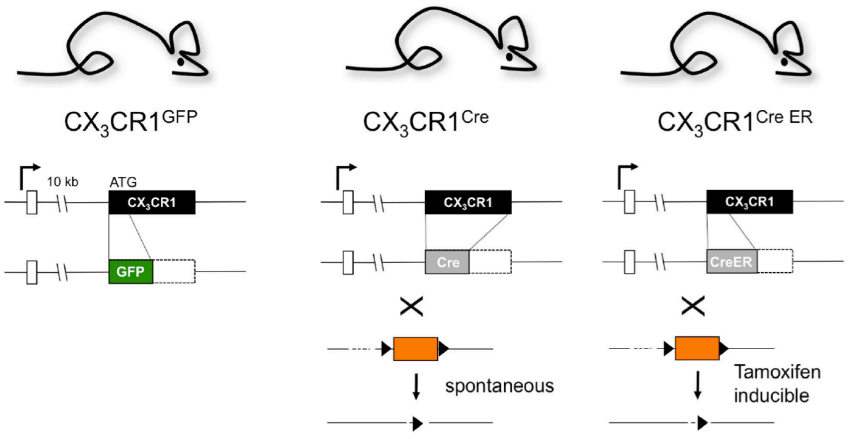

Scheme 7. The usage of CX$_3$CR1 promoter to target microglia and peripheral macrophages. Scheme of Cx3cr1^{Cre} and Cx3cr1^{CreER} systems, modified from [80]. Black triangles represent loxP sites.

2. Results

2.1 Microglia display a unique transcriptome and microRNA profile distinct from other tissue resident macrophages.

In order to reveal the miR signature of adult microglia, we performed an Agilent miR microarray analysis [83], comparing microglia with other tissue macrophages, such as colonic macrophages isolated from the large intestine and liver macrophages (Kupffer cells, KC) (**Fig. 1A**). Microglia displayed a set of 73 uniquely expressed miRs among these populations. These included miR-99a, miR-125b-5p, and miR-342-3p (**Fig. 1A**), which were recently shown to be induced by TGFβ treatment in cultured primary microglia [13]. In addition, we analyzed the transcriptiome of microglia using RNA sequencing and compared it to the ones of colonic and liver macrophages *(Lavin et al Cell 2014, in press)* (**Fig. 1B**). Interestingly, microglia uniquely expressed genes associated with neuronal development, such as *Nav2* [84], and *Sall1* [85]. Microglia also showed low expression of the *Cybb* gene encoding the neurotoxic factor Nox2 [86]. Notably, miRs predicted to target *Cybb*, miR-103-3p and miR-107-3p, were part of the miR cluster highly expressed in microglia (**Fig. 1A).** Microglia also highly expressed miR-146a-5p that was shown to down-regulate the NFkB pathway and reduce inflammatory response [74, 75]. In addition, microglia displayed high expression of miR-181b and miR-181c. MiR-181c was shown to down regulate the expression of TNFa and NO in a microglia cell-line in response to hypoxia, a stroke-like condition [77]. Mir-181b was shown to promote the activity of Matrix metalloproteinase 2 (MMP2) in cancer cell lines via its inhibition of *Timp3* [87]. MMPs are enzymes performing extracellular matrix (ECM) remodeling and are involved in various CNS pathologies, but also in physiological processes of neuronal development [88, 89]. Interestingly, *Mmp2* was highly expressed in microglia and colonic macrophages, as compared with Kupffer cells (**Fig. 1B)** and could possibly be dependent on miR-181b expression.

Overall these results show that microglia display a unique expression profile of miRs, which likely shapes their specific mRNA expression profile.

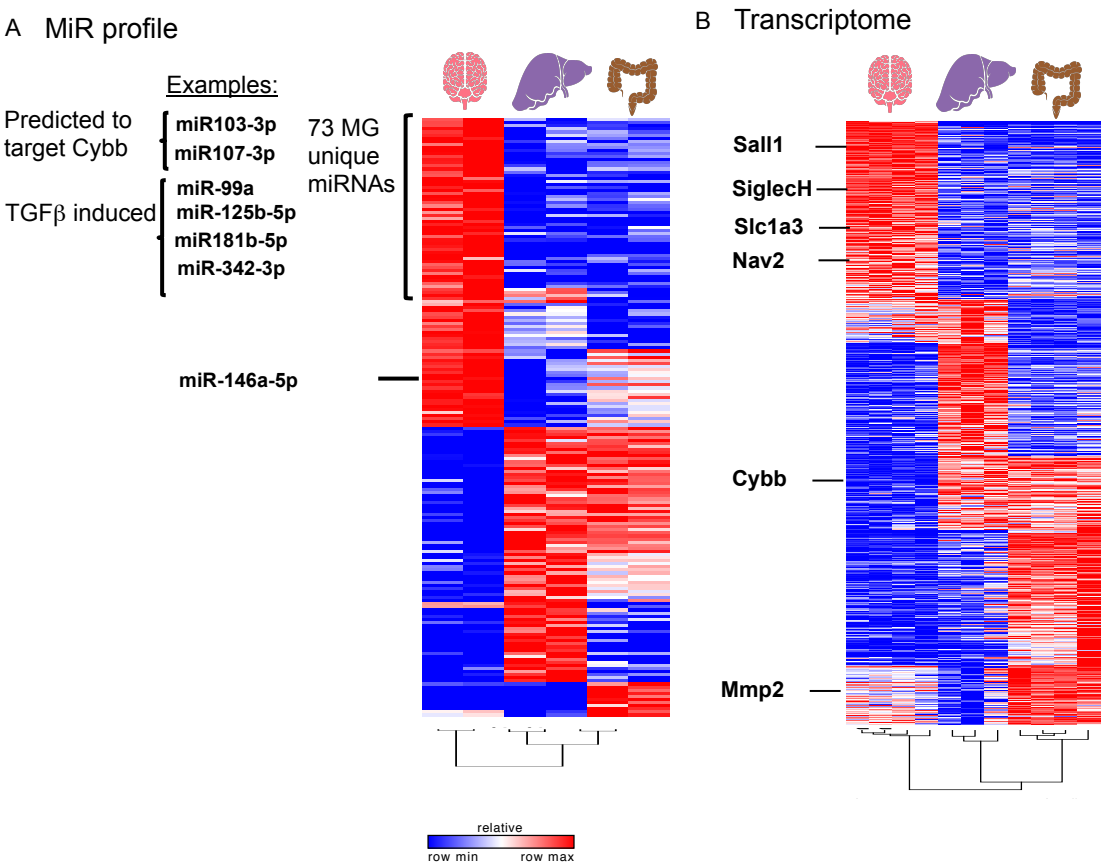

Figure 1. Microglia reveal a unique transcriptional and miR profile in comparison to other tissue resident macrophages.
(A) Heat map and hierarchical clustering for differentially expressed (FC, >2 or <-2; P<0.05) miRs between steady state microglia, liver macrophages, and colon macrophages, analyzed with agilent microarray. Intensity values were log-transformed, normalized and centered, and populations and genes clustered by pearson correlation test. Data are in duplicates; each replicate is a pool of 6 mice. (B) Heat map and hierarchical clustering for differentially expressed (FC, >2 or <-2; P<0.05) mRNAs between steady state microglia, liver macrophages, and colon macrophages, analyzed with RNA-seq approach. Read numbers were log-transformed, normalized and centered, and populations and genes clustered by pearson correlation. Number of replicates for each sample was; microglia (n=4), liver macrophages (n=3), and colon macrophages (n=4) with each replicate pooled from 6 mice. Statistical significance was measured with Anova.

2.2 Establishment of mice harboring a constitutive Dicer-deficiency in microglia.

In order to study the role of miRs in regulating homeostatic mechanisms governed by microglia, we generated mice harboring a deletion of *Dicer* in microglia. To this end we crossed *Cx3cr1*^{Cre} mice [80] and animals harboring a "floxed" *Dicer* allele [90], yielding *Cx3cr1*^{Cre}*:Dicer* $^{fl/fl}$ mice (**Fig. 2A**). To validate the conditional *Dicer* deletion in microglia, these cells were isolated from brains, sorted by FACS (**Fig. 2B**) and their genomic DNA and total RNA were purified. PCR analysis of the DNA for the Exon 24 deletion in *Dicer* alleles confirmed efficient rearrangements in microglia extracted from brains of *Cx3cr1*^{Cre}*:Dicer* $^{fl/fl}$ mice, but not *Dicer*$^{fl/fl}$ microglia (**Fig.**

2C). In addition, we performed a qRT-PCR analysis for three miRNAs highly expressed by WT microglia: miR-146a, known to regulate innate immunity [91], miR-142-3p, and miR200c. All these miRs showed a significant reduction in microglia isolated from *Cx3cr1*^{Cre}*:Dicer*$^{fl/fl}$ mice (**Fig. 2D**).

Taken together this confirms the *Dicer* gene deletion and lack of *Dicer* activity in microglia of *Cx3cr1*^{Cre}*:Dicer*$^{fl/fl}$ mice.

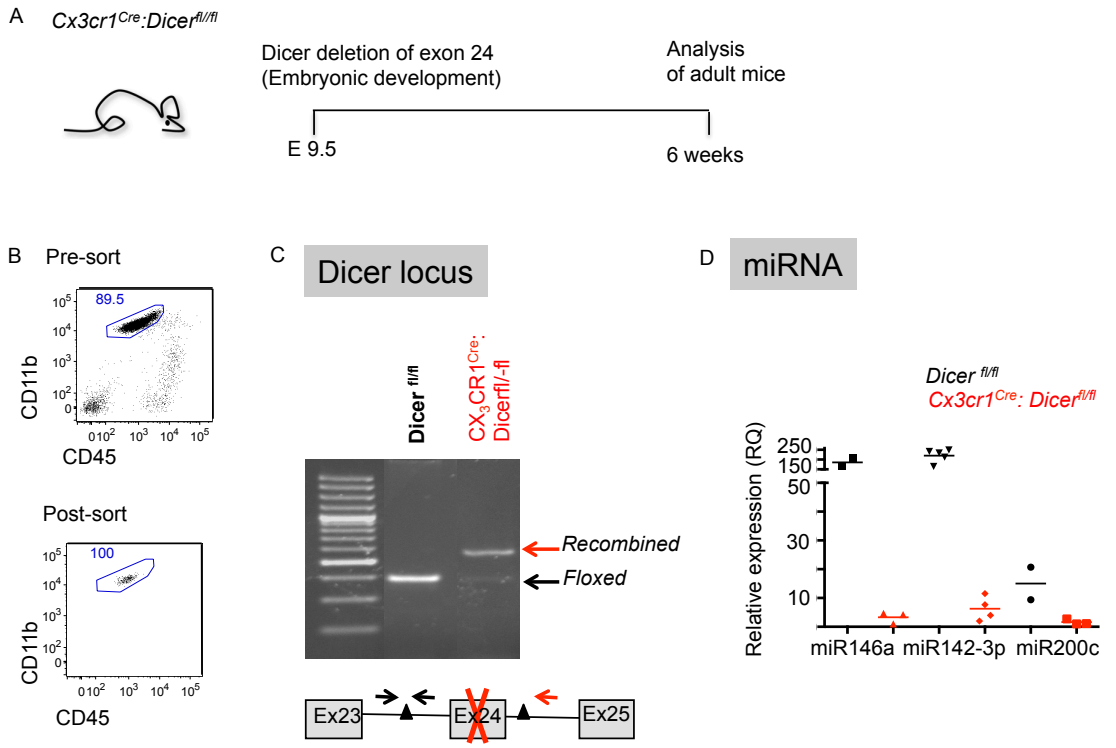

Figure 2. Cx3cr1*^{Cre}*:Dicer*$^{fl/fl}$ *mice show an efficient Dicer loss in microglia.
(A) A scheme describing the transgenic mouse model used for microglia dicer deletion and a time scale for analyzing dicer allel deletion efficiency. (B) Flow cytometry analysis images showing sorted brain microglia from either *Cx3cr1*^{Cre}*:Dicer*$^{fl/fl}$ or *Dicer*$^{fl/fl}$ mice pool (n=6 for each pool). Microglia were characterized as Ly6G^{neg}Ly6C^{neg}CD45^{int}CD11b^{+} cells. (C) Representative genomic PCR analysis image showing the PCR product for *Dicer* exon 24 deleted allele. Note that it appears only in *Cx3cr1*^{Cre}*:Dicer*$^{fl/fl}$ brain sorted Microglia. (D) Graphical summary showing qRT-PCR analysis for miR-146a, miR-142-3p and miR-200c expression within microglia sorted from brains of *Cx3cr1*^{Cre}*:Dicer*$^{fl/fl}$ or *Dicer*$^{fl/fl}$ mice. Data are expressed as mean +/- SEM, statistically analyzed with student T test (n=3 per group).

2.3 *Cx3cr1*^{Cre}*:Dicer*$^{fl/fl}$ mice display a reduced motoric function.

Cx3cr1^{Cre}*:Dicer*$^{fl/fl}$ mice were born at normal Mendelian frequencies and did not show gross developmental problems. At the age of 8 weeks, however, *Cx3cr1*^{Cre}*:Dicer*$^{fl/fl}$ mice started to display a motoric dysfunction, as indicated by their inability to spread their hind legs, when raised by their tails (data not shown). To further investigate and quantify the motoric activity of the animals, we subjected *Dicer*$^{fl/fl}$ and *Cx3cr1*^{Cre}*:Dicer*$^{fl/fl}$ mice to established locomotion tests (**Fig. 3A**), including an assay for hind limb function, hang-wire and rotarod motoric tests (**Fig. 3B, C**). All these assays for motoric functions revealed significant motoric impairment of *Cx3cr1*^{Cre}*:Dicer*$^{fl/fl}$ mice. Interestingly, the motoric impairment was not detectable before 8 weeks of age, although *Dicer* deletion in these mice occurs already at the stage of CX_3CR1^+ microglia precursors [80], which reside in the CNS at E9.5 [1, 4, 21]. Collectively, the above results demonstrate a late onset motoric deficiency due to *Dicer*-deficiency in microglia.

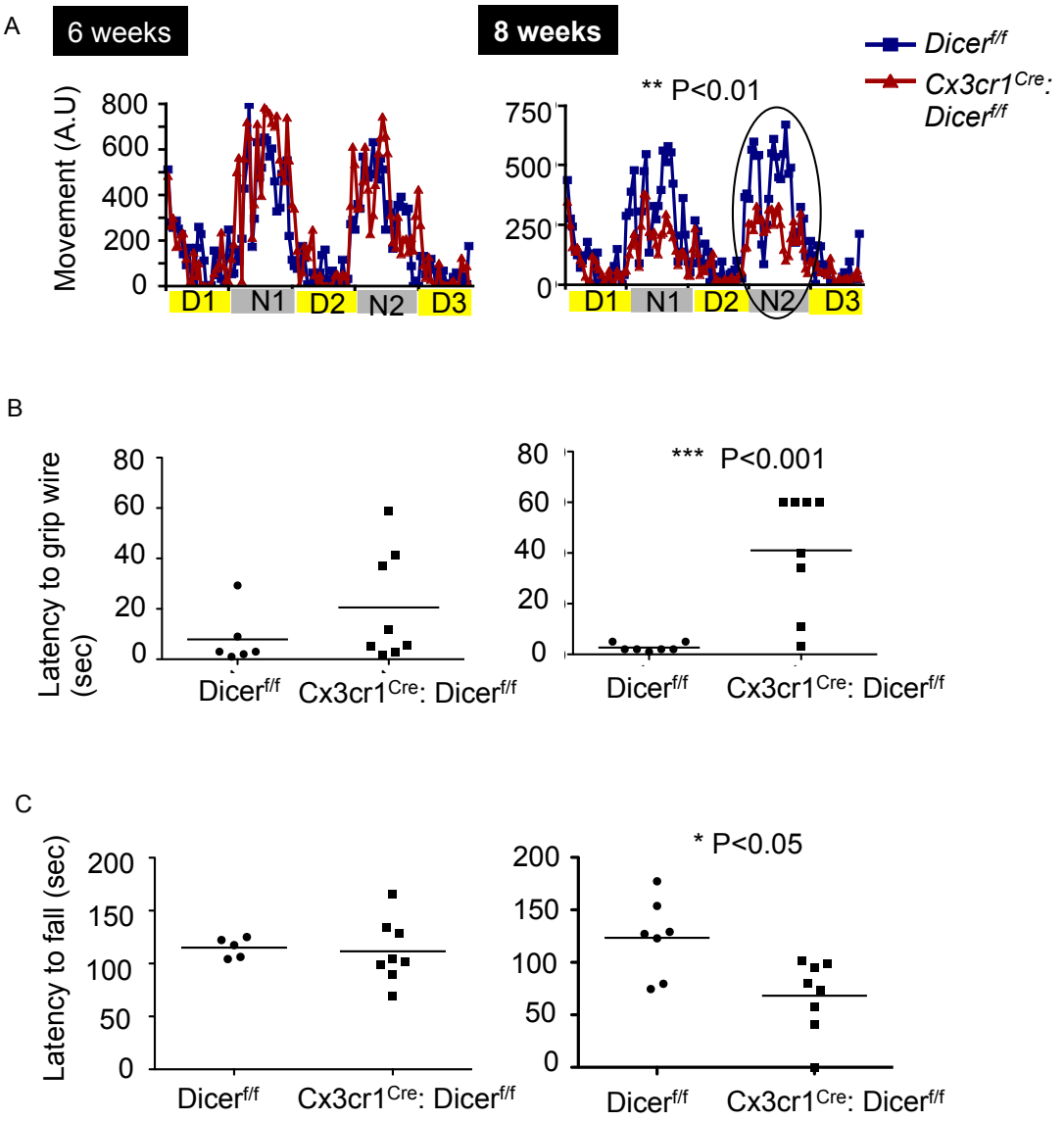

Figure 3. Cx3cr1^{Cre}:Dicer$^{fl//fl}$ mice show a reduced motoric function.
(A) Graphical summary showing home-cage locomotion during continuous periods of light (X-axis, marked in yellow) and dark (X-axis, marked in gray) showing that *Cx3cr1^{Cre}:Dicer$^{fl//fl}$* mice have reduced activity during dark period. (B) Graphical summary of hang-wire test showing that *Cx3cr1^{Cre}:Dicer$^{fl//fl}$* mice have longer latency to grip wire with hind legs. (C) Graphical summary of rotarod spinning wheel test showing that *Cx3cr1^{Cre}:Dicer$^{fl//fl}$* mice fall quicker from the rotarod. Locomotion test is plotted as average activity per group for each time point, statistically measured with repeated students T test. Hang-wire and rotarod data are displayed as mean +/- SEM, and statistically analyzed with students T test (6 weeks: n=5 and 8 for *Dicer $^{fl/fl}$* and *Cx3cr1^{Cre}:Dicer$^{fl//fl}$* mice, respectively; 8 weeks: n=7 and 8 for *Dicer $^{fl/fl}$* and *Cx3cr1^{Cre}:Dicer$^{fl//fl}$* mice, respectively).

2.4 Microglial *Dicer* deficiency results in astrocytosis at specific brain areas, related to motoric activity.

Given the neurologic deficiency of the *Cx3cr1*^{Cre}*:Dicer*$^{fl/fl}$ mice, we measured their brain sizes and weights. Eight week old mice though displaying motoric impairment, did not show any obvious changes in brain size or weight, however older mice (24 weeks) revealed reductions **(Fig. 4A, B)**. Next, the specific brain areas related to motoric behavior in mice, such as the motor cortex, cerebellum and brainstem, were examined for signs of reactive proliferating astrocytes, a process termed astrocytosis, and associated with neuronal damage due to trauma, infection, and neurodegenerative disease [92]. Sagittal sections of brainstems, cerebellum (Cb), and cortex **(Fig. 4C)** were examined by immunofluorescent labeling for the astrocyte-specific glial fibrillary acidic protein (GFAP). Interestingly, brainstem and cerebellum of *Cx3cr1*^{Cre}*:Dicer*$^{fl/fl}$ mice displayed astrocytosis, while the cortex was normal. Therefore, neuronal damage occuring specifically in brainstem and cerebellum might be related to the motoric impairment revealed in hind limbs.

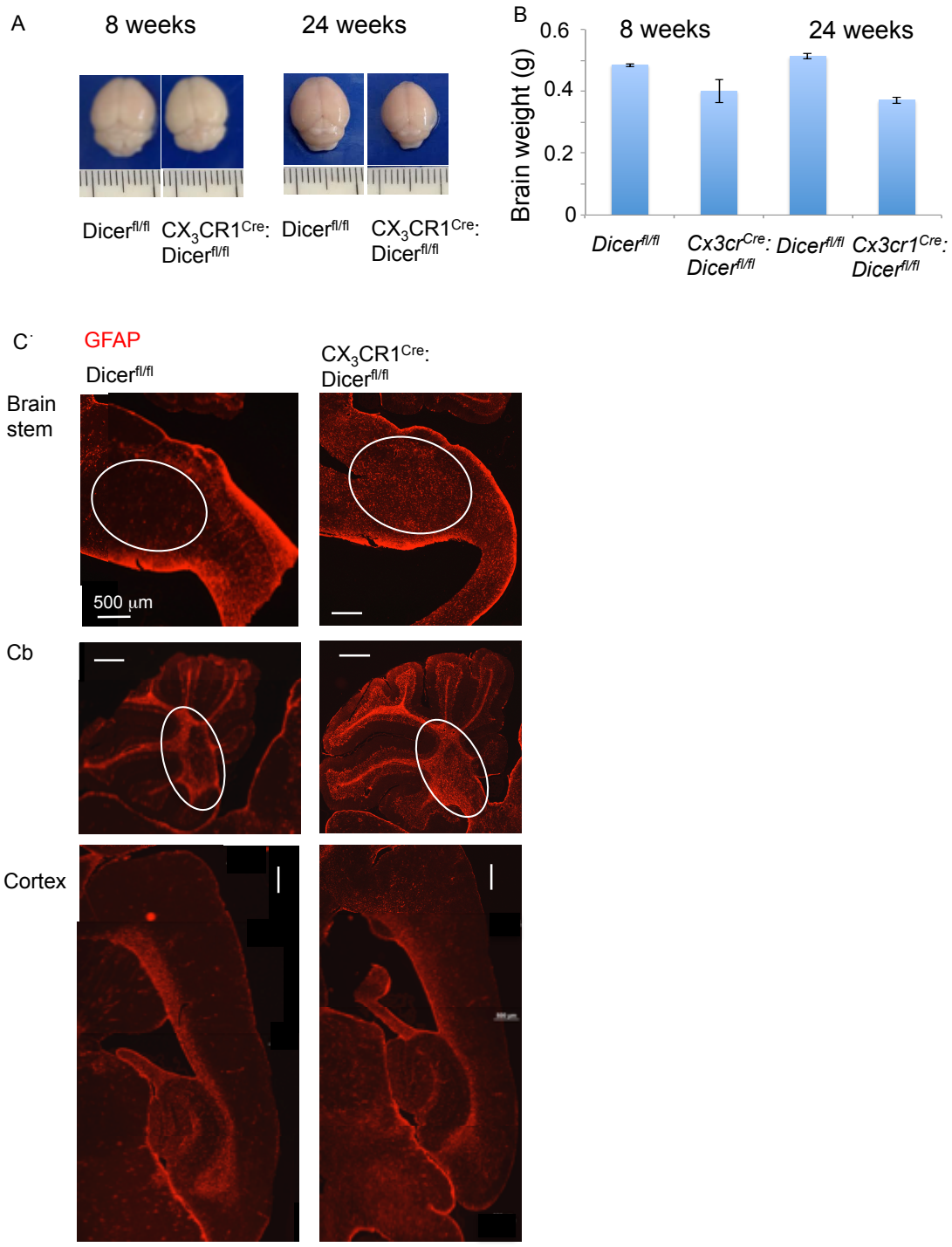

Figure 4. Cx3cr1^{Cre}:Dicer$^{fl//fll}$ mice show a reduced brain size and an appearance of astrocytosis in brainstem and cerebellum. (A) Representative pictures of whole brains isolated from 8 and 24 weeks old mice. (B) Graphical summary showing statistically significant reduction in brain weight in 24 weeks but not 8 weeks old *Cx3cr1^{Cre}:Dicer$^{fl//fl}$* mice (n=4 for both). Statistics was measured with students T test. (C) Representative pictures for GFAP staining (red) showing accumulated astrocytosis in brain-stem and cerebellum (Cb), but not cortex of 24 weeks old *Cx3cr1^{Cre}:Dicer$^{fl//fl}$* mice.

2.5 *Cx3cr1^{Cre}:Dicer $^{fl/fl}$* mice display astrocytosis, and reduced motor neuron numbers in the L5 ventral horn of the spinal cord.

Given their motoric deficiency of the hind limbs and the prominent astrocytosis in brainstem and cerebellum, we next screened the spinal cord (SC) lumbar 5 (L5) area of the *Cx3cr1^{Cre}:Dicer $^{fl/fl}$* mice, which innervates the hind limb musculature, for signs of pathology. GFAP staining revealed profound astrocytosis within the SC-L5 parenchyma of *Cx3cr1^{Cre}:Dicer $^{fl/fl}$* mice, already at 8 weeks of age, but not before (**Fig. 5A, B**).

Next, we analyzed motor neuron cell numbers using immunofluorescent staining for choline acetyl-transferase (ChAT) to probe for neuronal degeneration. The average number of motor neurons in the ventral horn was calculated from 10 consecutive sections covering the whole L5 area of the SC. Fluorescent microscopy analysis revealed a significant 30-40% reduction of motor neurons within the L5 of *Cx3cr1^{Cre}:Dicer $^{fl/fl}$* mice compared to littermate controls at 24 weeks, but not 8 weeks (**Fig. 6A, B).** Caspase-3 staining for apoptosis, revealed the presence of apoptotic motor neurons within the L5-SC of *Cx3cr1^{Cre}:Dicer $^{fl/fl}$* mice at 8-12 weeks of age (**Fig. 6 C, D)**.

The results above demonstrate an accumulative damage occurring in the SC-L5 of *Cx3cr1^{Cre}:Dicer $^{fl/fl}$* mice, including prominent astrocytosis at the age of 8 weeks and a reduction in the number of ventral horn motor neurons by 24 weeks of age.

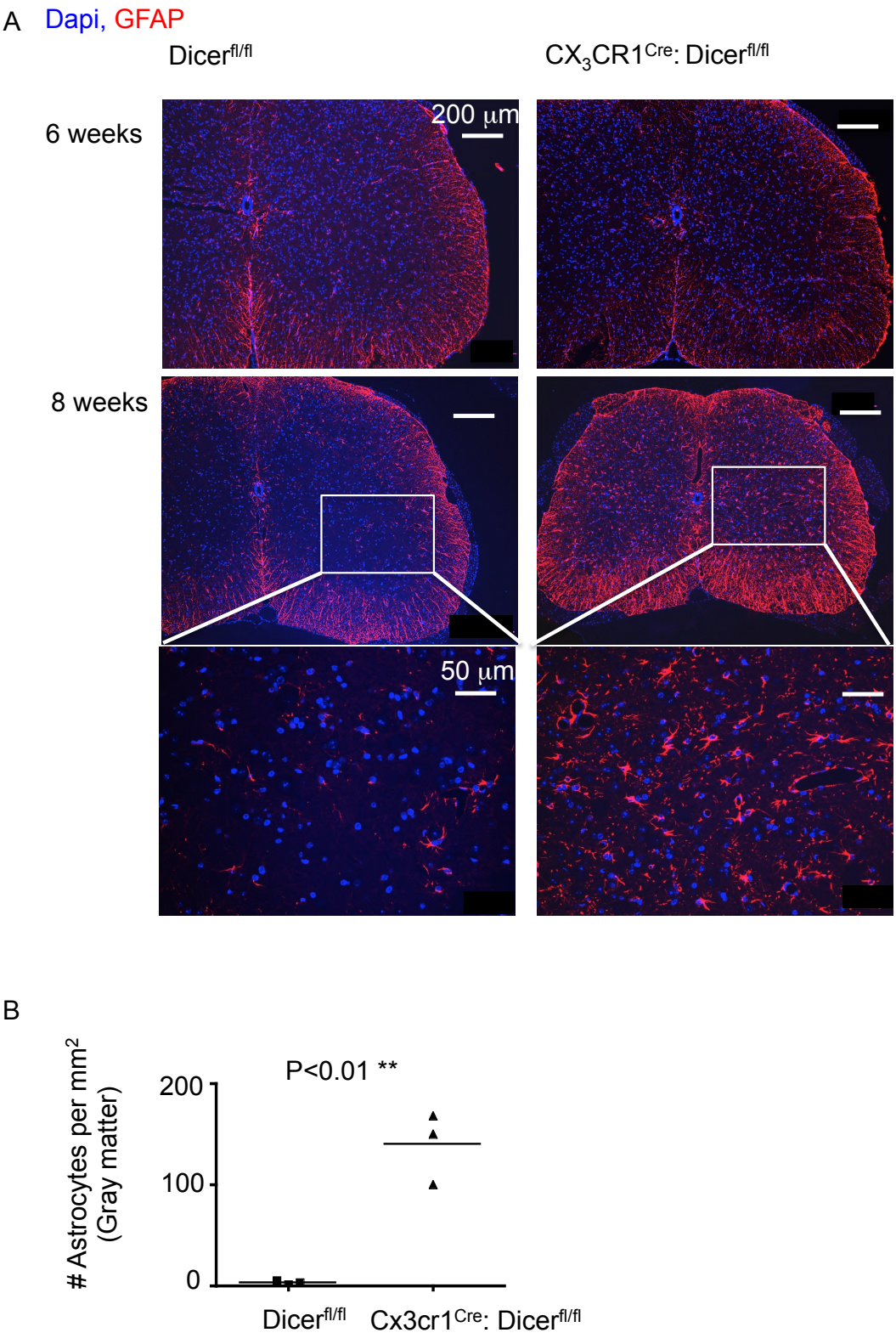

Figure 5 Cx3cr1^{Cre}:Dicer$^{fl/fl}$ mice display astrocytosis in the L5-SC.
(A) Representative immunofluorescent images of SC-L5 area from *Dicer$^{fl/fl}$* versus *Cx3cr1^{Cre}:Dicer$^{fl/fl}$* mice showing astrocyte specific staining with anti GFAP (red), in addition to nuclei Dapi counterstaining (blue). (B) Graphical summary showing that astrocyte number per mm^2 area (n=3, per group) is increased in *Cx3cr1^{Cre}:Dicer$^{fl/fl}$* mice.

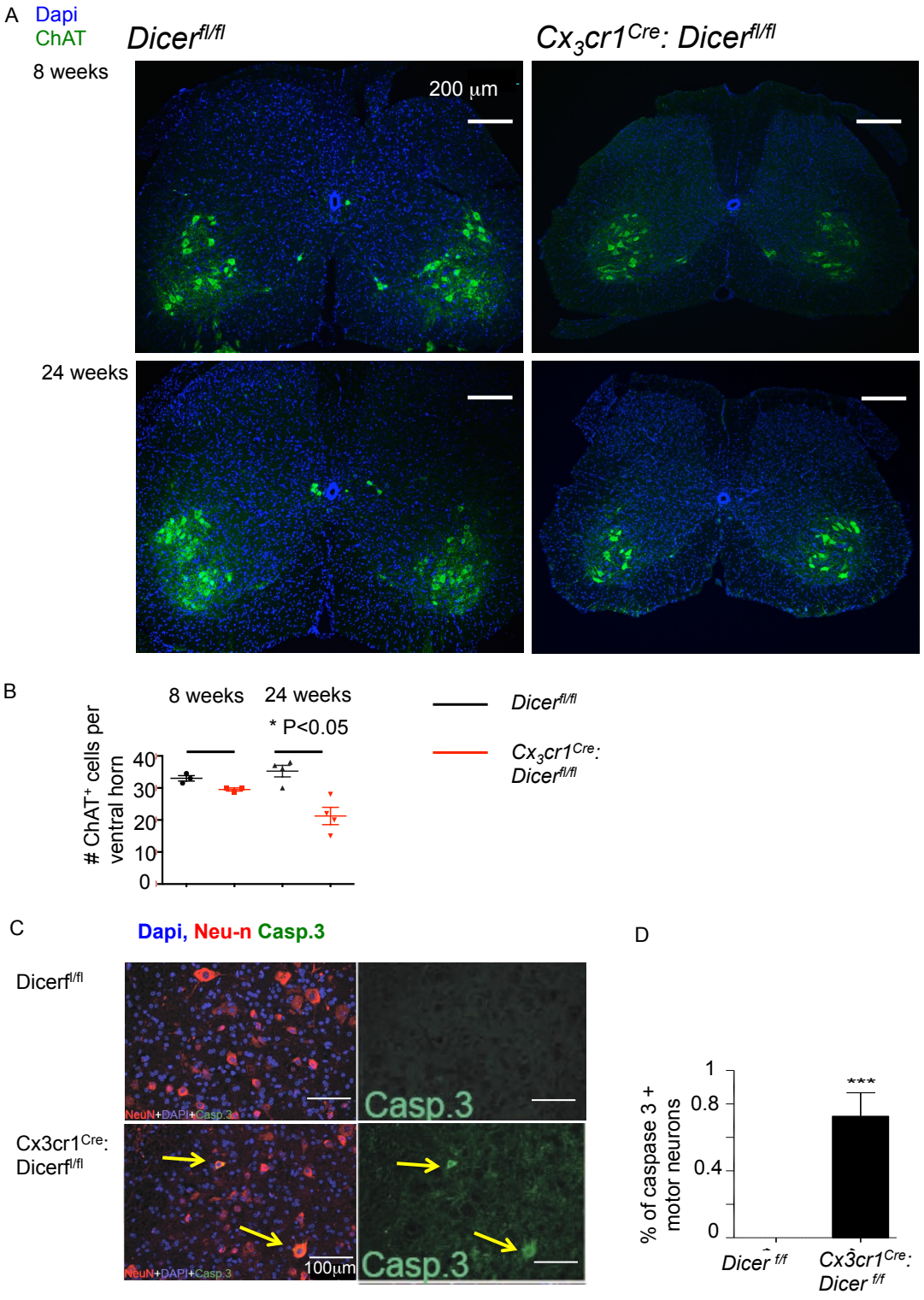

***Figure 6. Cx3cr1^{Cre}:Dicer$^{fl/fl}$* mice display reduced motor neurons number in the SC-L5 area.**
(A) Representative immunofluorescent images of SC-L5 area from *Dicer$^{fl/fl}$* versus *Cx3cr1^{Cre}:Dicer$^{fl/fl}$* 8 weeks and 24 weeks old mice, showing motor neuron specific staining with anti ChAT (green), in addition to nuclei Dapi counterstaining (blue). (B) Graphical summary showing that motor neuron number per mm^2 area (n=4, per group) is decreased in 24 weeks but not 8 weeks old *Cx3cr1^{Cre}:Dicer$^{fl/fl}$* mice. (C) Representative immunofluorescent images of SC-L5 area from *Dicer$^{fl/fl}$* versus *Cx3cr1^{Cre}:Dicer$^{fl/fl}$* mice showing staining for apoptotic neurons labeled with the neuronal marker-Neu-n (red), apoptosis marker-cleaved caspase-3 (green), and nuclei counterstaining-Dapi (blue). Arrows

highlight Neu-n^{+}Caspase3^{+} apoptotic neurons. (n=3, per group). (D) Graphical summary showing an increase in apoptotic motor neuron number per mm^{2} in *Cx3cr1^{Cre}:Dicer$^{fl/fl}$* mice (n=3, per group). Quantitative data for all experiments here are expressed as mean +/- SEM and statistically analyzed with students T test (P value represented by * <=0.05, ** <= 0.01, or *** <=0.001).

2.6 *Cx3cr1^{Cre}:Dicer $^{fl/fl}$* mice show an accumulation of Mac2^{+} phagocytic cells and a reduced number of axons in L5- ventral root.

The innervation of leg muscles occurs via the sciatic nerve, which is composed from the L4 and L5 motor neuron axonal roots (ventral roots). The sciatic nerve originates in the CNS, but most of the nerve is located in the peripheral nervous system (PNS). Therefore damage in either compartment could be harmful to its integrity and impair hind limb motorics. L5 axonal root degeneration is a known feature of neurodegenerative diseases, such as ALS, commonly seen in human patients and the mSOD1 mouse model [93, 94], even prior to L5 motor neurons loss [94]. Sciatic nerve degeneration triggers a regenerative process, which involves Schwann cells and/or infiltrating macrophages that phagocytose myelin debris shed from damaged axons [95]. Both cell types express the galactose specific lectin galectin-3, also named Mac-2 [96], a molecule functionally important for myelin phagocytosis following axonal injury as demonstrated in *Mac2* deficient mice [96]. In order to probe for potential axonal damage in *Cx3cr1^{Cre}:Dicer $^{fl/fl}$* mice, we specifically excised L5 ventral roots and performed a staining for ChAT and Mac2. We observed a prominent accumulation of Mac2^{+} cells specifically in *Cx3cr1^{Cre}:Dicer $^{fl/fl}$* mice of all age groups tested, including time points before the onset of motoric impairment (6 weeks) **(Fig. 7A**). Motor axon numbers per L5 root were reduced in later stages (24 weeks) **(Fig. 7B),** similarly to late occurring motor neuron cell body loss **(Fig. 6A, B**). Collectively, these results show that *Dicer* deficient microglia cause axonal damage in the SC-L5 ventral roots.

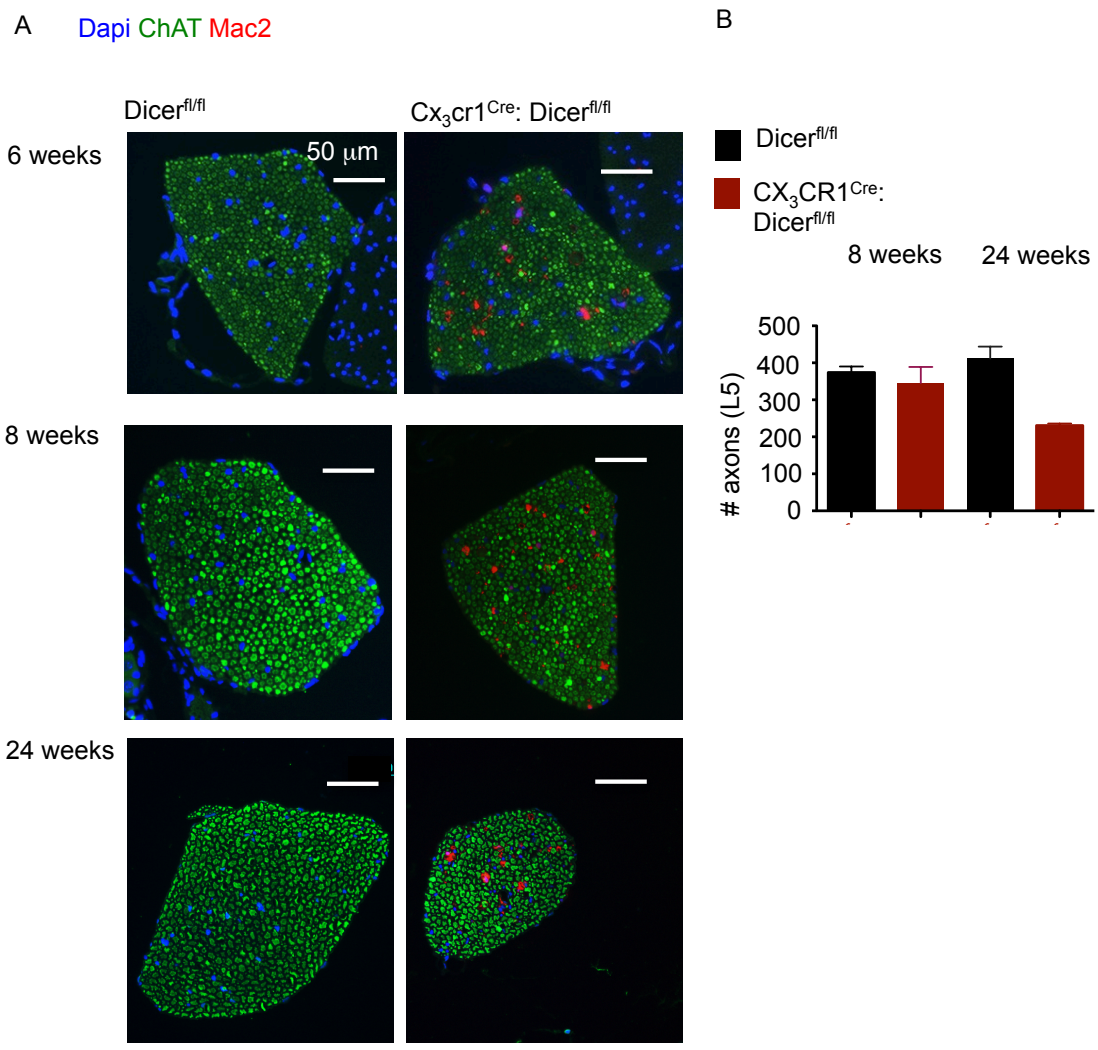

Figure 7. Cx3cr1^{Cre}:Dicer$^{fl//fl}$ mice show increased incidence of Mac2^{+} phagocytic cells in L5 ventral roots and reduction of overall axonal number per root.

Representative immunofluorescent images of SC-L5 ventral root cross sections, isolated from either *Dicer$^{fl/fl}$* or *Cx3cr1^{Cre}:Dicer$^{fl/fl}$* at the age of 6, 8 and 24 weeks (A), motor axons are labeled with ChAT (green), phagocytic cells are labeled with Mac2 (red). (B) Graphical summary of 8 and 24 weeks old mice axonal number per root, showing reduced number of axons in 24 weeks old *Cx3cr1^{Cre}:Dicer$^{fl/fl}$* mice. All data are expressed as mean +/- SEM. (n=3, in 8 weeks and 24 weeks old mice). Statistical analysis was performed with Students T test.

2.7 Histological evaluation of *Cx3cr1^{Cre}:Dicer $^{fl/fl}$* microglia reveals their activation and increased turnover.

2.7.1 Dicer-deficient microglia show an activated phenotype.

In order to evaluate the activation state of the *Dicer*-deficient microglia, we performed an immunofluorescent staining for the microglia marker Iba1(ionized calcium-binding adapter molecule 1) on sections of cortex, cerebellum and SC of 8 week old *Cx3cr1^{Cre}:Dicer $^{fl/fl}$* and littermate *Dicer$^{fl/fl}$* mice. Fluorescent microscopic imaging revealed a typical ramified morphology for *Dicer$^{fl/fl}$* microglia. In contrast, microglia of *Cx3cr1^{Cre}:Dicer $^{fl/fl}$* mice exhibited amoeboid shapes and increased cell body sizes (**Fig. 8A**). Quantitative morphometric analysis of 3D-reconstructed images of single microglia cells revealed additional features, such as reduced dendrite length and branching (**Fig. 8B, C**). SC sections were also stained for the activation marker CD68, which is associated with microglia polarization towards a pro-inflammatory phenotype [50]. Sections were taken from tissues of 4-6 weeks old mice, a period before obvious impaired motoric phenotype, in an attempt to separate intrinsic changes of the mutant microglia from microglial responses to neuronal damage. *Cx3cr1^{Cre}:Dicer $^{fl/fl}$* mice displayed elevated expression of CD68 (**Fig. 8D**). CD68 expression was also evaluated by flow-cytometry, alongside with MHCII and the co-stimulatory molecule CD86. All these markers were found to be increased in 4-6 weeks old *Cx3cr1^{Cre}:Dicer $^{fl/fl}$* mice, as compared to littermate controls (**Fig. 8E)**. Collectively, these results show that a *Dicer* deficiency of microglia results in microglia activation and the expression of markers associated with inflammation.

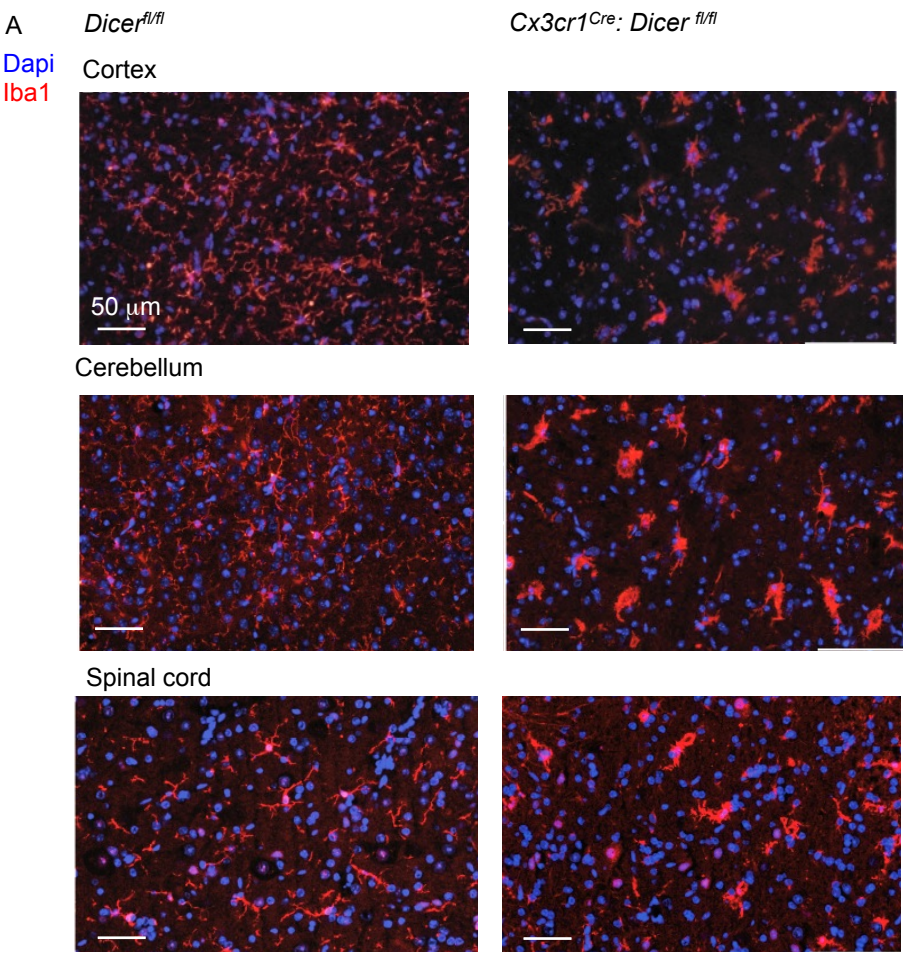
A
Dapi
Iba1
Dicer fl/fl
Cx3cr1 Cre: Dicer fl/fl
Cortex
50 μm
Cerebellum
Spinal cord

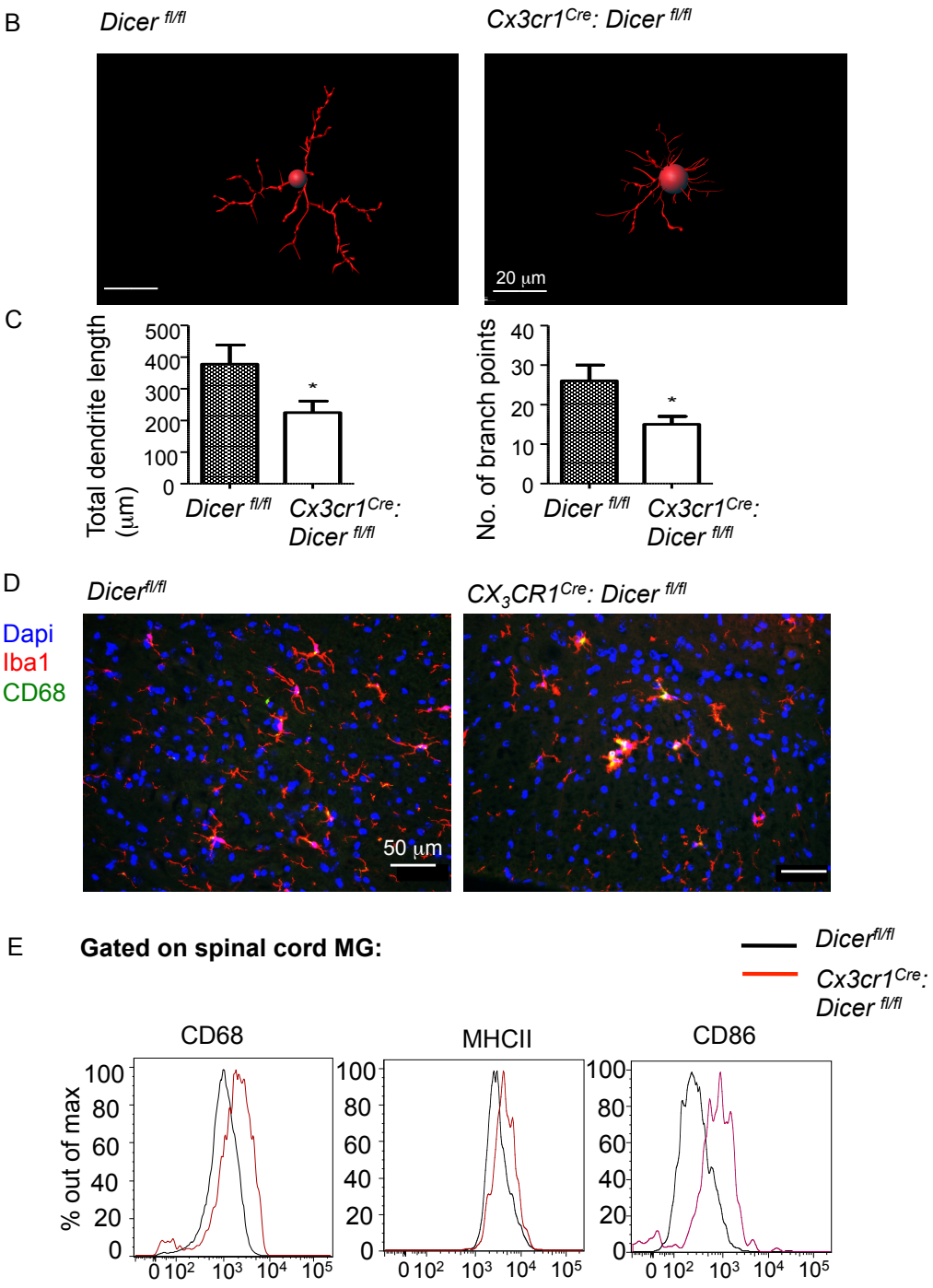

Figure 8. Cx3cr1^{Cre}:Dicer$^{fl//fl}$ microglia show an activated phenotype. (A) A representative fluorescent microscopic images of paraffin sections of motor cortex, cerebellum and SC tissues extracted from 8 weeks old *Dicer$^{fl/fl}$* or *Cx3cr1^{Cre}:Dicer$^{fl//fl}$* mice showing staining for Iba1 (red) and Dapi (blue). (B, C) Quantitative morphometric analysis of 3D-reconstructed images of single Microglia cells, isolated from 8 weeks old mice, showing dendrite length and number of branches. (n=3 of both *Dicer$^{fl/fl}$* and *Cx3cr1^{Cre}:Dicer$^{fl//fl}$*). (D) Representative fluorescent microscopic images of paraffin sections of SC-L5 area, extracted from 4 weeks old *Dicer$^{fl/fl}$* or *Cx3cr1^{Cre}:Dicer$^{fl//fl}$* mice showing staining for Dapi (blue), Iba1 (red), and CD68 (green). (E) Flow cytometry analysis images showing expression of CD68, MHCII and CD86 co-stimulatory molecules in SC microglia isolated from 4-6 weeks old *Cx3cr1^{Cre}:Dicer$^{fl//fl}$* and *Dicer$^{fl/fl}$* mice (n=6 and n=5 respectively). For all results here, data are expressed as mean +/- SEM, statistically analyzed with student T test (P value represented by * <=0.05, or ** <= 0.01).
The above immunohistochemistry was done in collaboration with Dr. Thomas Blank from the lab of Prof. Marco Prinz, Universitats klinikum Freiburg.

2.7.2 Dicer-deficient microglia display increased cell proliferation and apoptosis.

Microglia activation during challenge is associated with their increased proliferation, followed by apoptosis at the disease resolution stage [97]. *Dicer* deficiency was shown to promote apoptosis in epidermal resident $CD11c^{+}$ cells (i.e., Langerhans cells, LC), using a $CD11c^{Cre}$:$Dicer^{fl/fl}$ mouse model [98]. Therefore, we decided to explore both proliferation and apoptosis in $Cx3cr1^{Cre}$:$Dicer^{fl/fl}$ microglia. To examine microglial proliferation in the SC-L5 area we stained for the intra-cellular proliferation marker Ki67, present only during active phases of cell cycle. Microscopy analysis revealed an increased number of cells positive for both Iba1 and Ki67 among the *Dicer*-deficient microglia (**Fig. 9A, B**). To assess the apoptosis rate, we performed a terminal deoxynucleotidyl transferase (TdT)-mediated dUTP nick end labeling (TUNEL). Analysis revealed the presence of apoptotic $TUNEL^{+}$ $Iba1^{+}$ *Dicer*-deficient microglia (**Fig. 9C, D**). Furthermore, the number of $Iba1^{+}$ microglia cells was reduced in SC of 6-month old $Cx3cr1^{Cre}$:$Dicer^{fl/fl}$ mice (**Fig.10E, F**). Collectively, these results suggest that the Dicer-deficiency in microglia results in an increased turnover, manifested in increased proliferation and apoptosis, culminating in a progressive reduction of microglia cells with age.

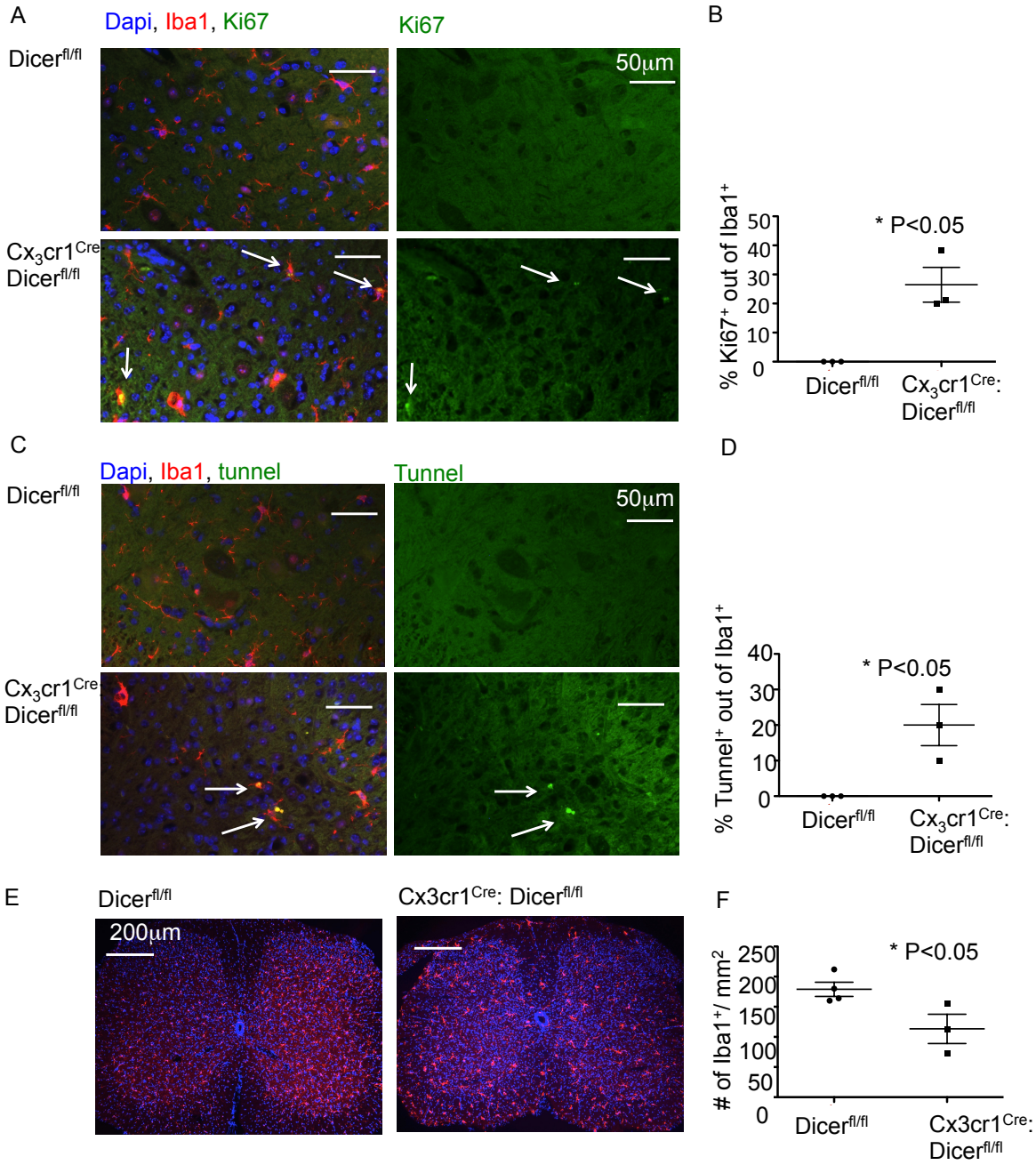

Figure 9. Increased proliferation and apoptosis rate, in addition to age dependent frequency reduction of Cx3cr1^{Cre}:Dicer$^{fl/fl}$ microglia. (A) Representative immunofluorescent images of SC-L5 area from *Dicer$^{fl/fl}$* versus *Cx3cr1^{Cre}:Dicer$^{fl/fl}$* mice. Paraffin sections were stained with Dapi (blue), Iba1 (red), and Ki67 (green). Arrows highlight Iba1^{+}Ki67^{+}cells. (B) Graphical summary showing the percentage of Ki67^{+} events out of Iba1^{+} Microglia cells (n=3 per group). (C) Representative immunofluorescent images of SC-L5 area from *Dicer$^{fl/fl}$* versus *Cx3cr1^{Cre}:Dicer$^{fl/fl}$* mice. Paraffin sections were stained with Dapi (blue), Iba1 (red), and TUNEL (green). Arrows highlight Iba1^{+}TUNEL^{+} apoptotic Microglia cells. (D) Graphical summary showing the percentage of TUNEL^{+} events out of Iba1^{+} microglia cells (n=3 per group). (E) Representative immunofluorescent images of SC-L5 area from 6-month old *Dicer $^{fl/fl}$* versus *Cx3cr1^{Cre}:Dicer$^{fl/fl}$* mice. Floating sections were stained with Dapi (blue) and Iba1 (red). (H) Graphical summary showing the number of Iba1^{+} Microglia cells per area. Data for all experiments here are expressed as mean +/- SEM and statistically analyzed with students T test (P value represented by * <=0.05, or ** <= 0.01). The above immunohistochemistry was done in collaboration with Dr. Thomas Blank from the lab of Prof. Marco Prinz, Universitats klinikum Freiburg.

2.8 Microarray analysis of the mRNA of *Dicer*-deficient microglia reveals their activation and loss of unique homeostatic gene signature.

To identify molecular pathways controlled by miRs in microglia we performed an Affymetrix microarray chip analysis of microglia sorted fro m *Dicer*$^{fl/fl}$ and*Cx3cr1*^{Cre}*:Dicer* $^{fl/fl}$ brains and SC. Six weeks old mice were analyzed in order to reveal differences between *Dicer*$^{fl/fl}$ and *Cx3cr1*^{Cre}*:Dicer* $^{fl/fl}$ microglia prior to motoric phenotype (onset at 8 weeks), and reduce a secondary impact of neuronal damage **(Fig. 10A)**. *Cx3cr1*^{Cre}*:Dicer* $^{fl/fl}$ microglia from brain and SC shared common differentially expressed genes (248), i.e. 30% out of all differentially expressed genes (794). The rest of the differentially expressed genes were divided into brain only (396) and SC only sets (150). These differentially expressed genes found exclusively in *Cx3cr1*^{Cre}*:Dicer* $^{fl/fl}$ brain and SC might reflect differences between microglia in these specific CNS compartments [99].

Common differentially expressed genes in brain and SC of *Cx3cr1*^{Cre}*:Dicer* $^{fl/fl}$ microglia could be divided into 190 upregulated and 58 downregulated genes **(Fig. 10B)**, and were functionally categorized according to GO annotations. Upregulated genes fell into the following groups: *neurotoxicity and ROS*, *immune mediators*, *PRR, cytokines*, *complement signaling, apoptosis, cell division, ECM, and cell motility* **(Fig. 10C).** The "*ROS production*" cluster was particularly relevant to microglia neurotoxicity, especially with respect to the pro-inflammatory oxidase Nox2 (*Cybb*), a key component in generation of reactive oxygen species [100]. Another upregulated gene associated with generation of ROS is *Xdh*, which was reported to be increased in mSOD1 microglia associated with ALS [12]. The "*immune mediators*" cluster contains genes related to microglia/ macrophage activation. It includes *Trem1* and *Trem3*, which amplify innate inflammatory response [101]. The upregulated genes *S100a8* and *S100a9* are members of the S100-protein family performing calcium-binding acivity and have lately been identified as important endogenous DAMPs, secreted as a complex by activated phagocytes and recognized by TLR4 [102]. Of note, *S100a8* and *S100a9* were reported to be increased in brain microglia associated with various neurological disorders [103, 104]. *Lcn2* is a member of the lipocalin family, and is involved in innate immunity by sequestering of iron and limiting bacterial growth [105]. Interestingly, Lipocalin-2 promotes neuronal death [106], and regulates activation and ameboid morphology transformation of microglia [107, 108]. Lastly,

Spp1 (Osteopontin) was proposed to be neurotoxic since it contributed to disease progression in EAE [109] and increased in mSOD1 microglia, but was also shown to have a neuroprotective role in a model of spinal cord injury (SCI) [110]. Downregulated genes were categorized by the GO analysis into *"Neuronal development and function", "ECM",* and genes recently identified as "*steady state microglia signature*" [13]. Interestingly, the "*neuronal development*" cluster contained *Nav2*, which was shown to promote neurite outgrowth in SC and hindbrain during development [111]. An additional downregulated gene involved with the control of neuronal function is GLAST (*Slc1a3*), a glutamate transporter required for clearance of access extracellular glutamate and prevention of neuronal damage [112, 113]. Overall, *Dicer*-deficient microglia become activated with increased expression of genes related to inflammatory response and neurotoxicity. This is in line with other neurodegenerative models, such as the SOD1 ALS model [12]. In addition *Dicer*-deficient microglia displayed decreased expression of genes related to neuronal development.

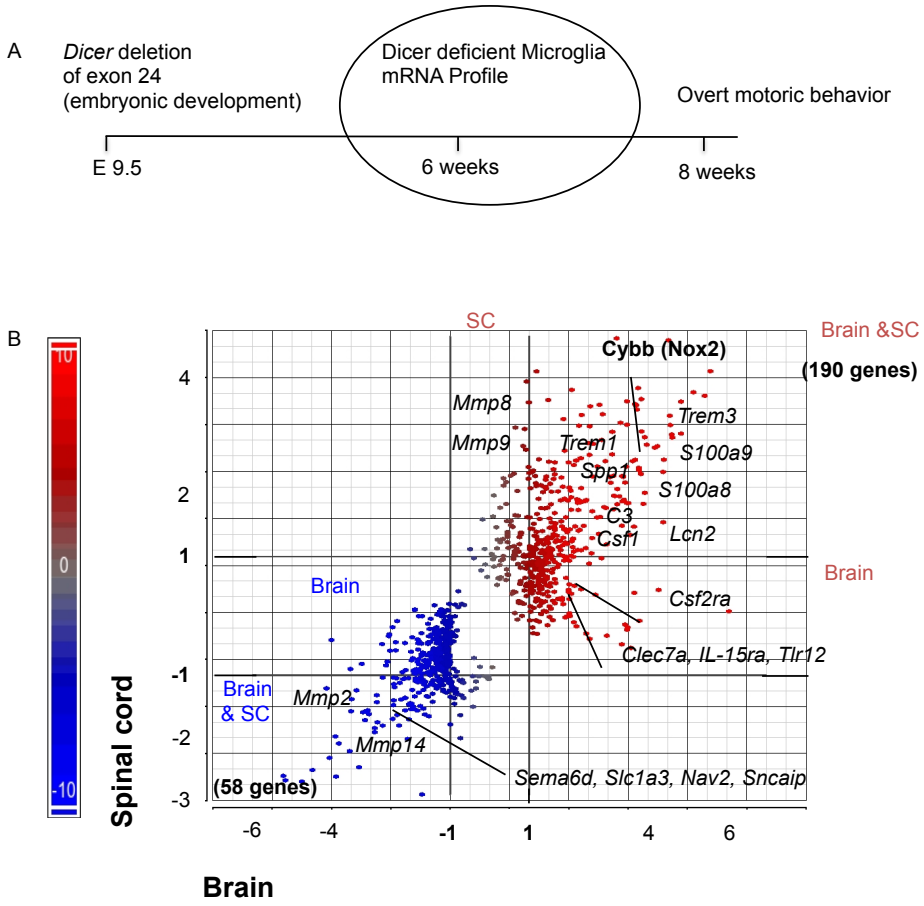

Figure 10 (A-B). Cx3cr1^{Cre}:Dicer$^{fl//fl}$ microglia increase pro-inflammatory & neurotoxic factors.
(A) Time scale showing microglia were isolated at 6 weeks, prior to obvious motoric impairments. (B) A scatter plot showing differentially expressed mRNA (FC, >=2 or =<-2; P=<0.05) in *Cx3cr1^{Cre}:Dicer$^{fl//fl}$* microglia isolated from either Brain (X axis) or SC (Y axis). mRNA expression was analysed with ST1 affymetrix microarray. Intensity values were normalized and the log difference between *Cx3cr1^{Cre}:Dicer$^{fl//fl}$* and *Dicer$^{fl/fl}$* of differentialy expressed genes is displayed. Number of replicates was; brain n=2 (both *Dicer$^{fl/fl}$* and *Cx3cr1^{Cre}:Dicer$^{fl//fl}$*), and SC n=3 (both *Dicer$^{fl/fl}$* and *Cx3cr1^{Cre}:Dicer$^{fl//fl}$*), with each replicate pooled from 6-8 mice. Statistical significance test was performed with Anova.

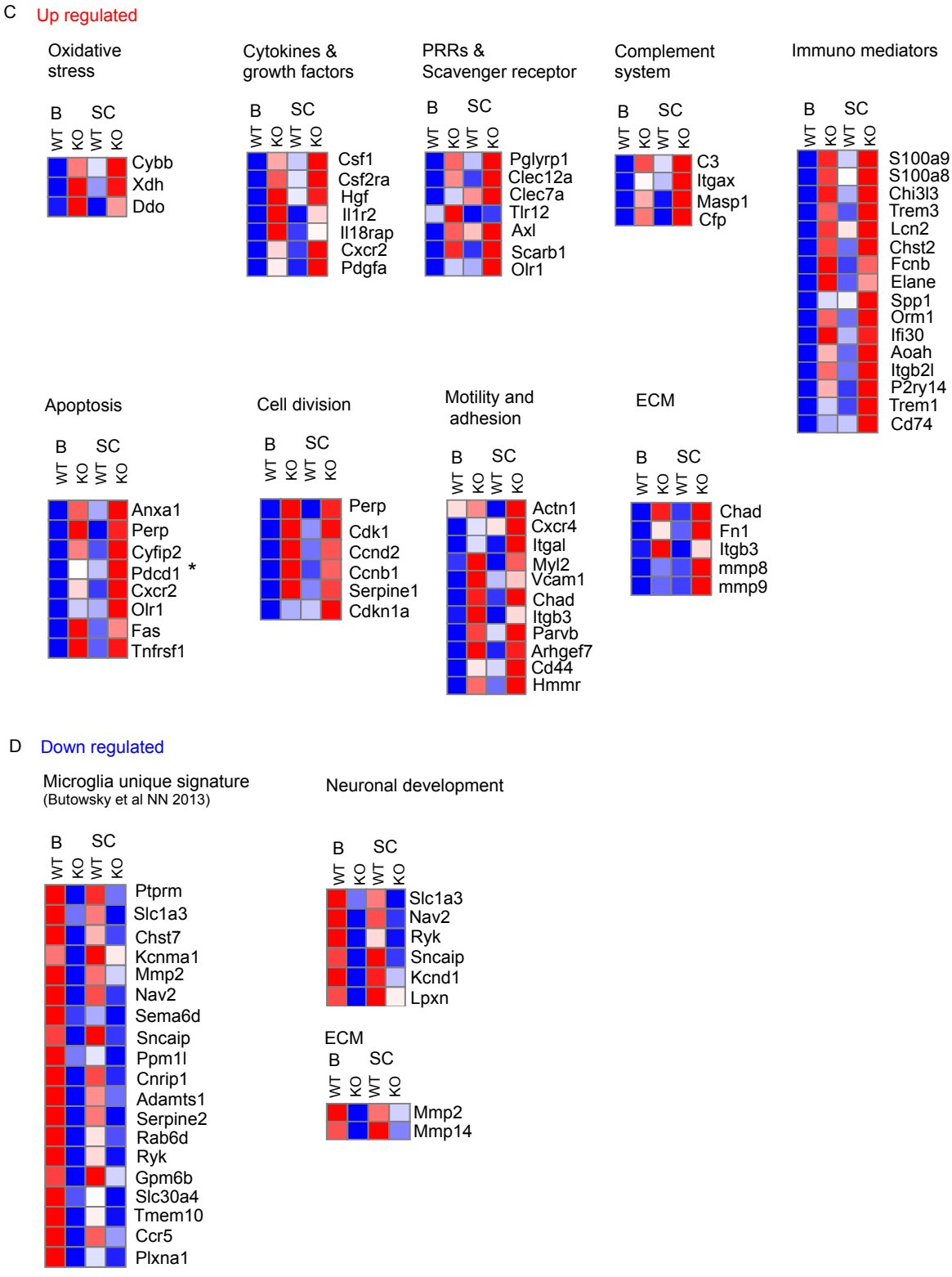

Figure 10 (C-D). Functional categorization of differentially expressed genes in Cx3cr1^{Cre}:Dicer$^{fl/fl}$ (KO) Microglia. (C) A Heat map displaying functional clustering according to GO annotations of significantly Up regulated genes (P<0.05, FC>2), in *Cx3cr1^{Cre}:Dicer$^{fl/fl}$* (KO) Vs. *Dicer$^{fl/fl}$* (WT) microglia. (D) A Heat map displaying functional clustering according to GO annotations of down regulated genes (P<0.05, FC<-2), of *Cx3cr1^{Cre}:Dicer$^{fl/fl}$* (KO) Vs. *Dicer$^{fl/fl}$* (WT) microglia. Colors represent signal intensity values derived from affymetrix microarray platform. Number of replicates was; brain n=2 (both WT and KO), and SC n=3 (both WT and KO), with each replicate pooled from 6-8 mice. Statistical significance test was performed with Anova.

2.9 Reconstitution of *Dicer*-deficient microglia by BM-derived WT brain macrophages does not rescue the motoric-deficiency.

Lethal irradiation and subsequent complementary bone marrow (BM) transfer results in full reconstitution of peripheral BM-derived hematopoietic cells, but replaces only 10-15% of the microglia compartment [14, 93]. Under specific disease conditions a more efficient reconstitution and functional rescue of impaired microglia has been reported. Thus, transfer of WT BM into 4 week old *Mecp2*$^{-/-}$ hosts, a murine Rett syndrome model associated with diverse neurological deficits and pre-mature death, was reported to result in long-term engraftment of the brain parenchyma by BM-derived microglia-like cells and arrest of disease development [114].

To examine if we can rescue *Cx3cr1*^{Cre}*:Dicer*$^{fl/fl}$ mice from the progressive motor neuron deficiency we transferred CD45.1^{+} WT BM into lethally irradiated CD45.2^{+} *Cx3cr1*^{Cre}*:Dicer*$^{fl/fl}$ recipients generating (WT > *Cx3cr1*^{Cre}*:Dicer*$^{fl/fl}$) BM chimeras and as a control, we transferred CD45.1^{+} WT BM into CD45.2^{+} WT recipients, generating (WT > WT) BM chimeras. In addition, we wished to elucidate if *Dicer*-deficient monocyte-derived macrophages (also targeted in the *Cx3cr1*^{Cre}*:Dicer*$^{fl/fl}$ mice) would contribute to the disease via damage to central or peripheral nervous system. For that purpose we generated *Cx3cr1*^{Cre}*:Dicer*$^{fl/fl}$*: RosaYfp* BM transfer into CD45.1^{+} WT recipients (*Cx3cr1*^{Cre}*:Dicer*$^{fl/fl}$*: RosaYfp* > WT). Of note, the Mac2^{+} cells found in L5 motoric roots of *Cx3cr1*^{Cre}*:Dicer*$^{fl/fl}$ mice (**Fig. 7**), have been reported in other systems to be partially comprised of infiltrating peripheral macrophages [95, 96]. In addition, we generated *Cx3cr1*^{Cre}*:Dicer*$^{fl/fl}$*: RosaYfp* BM transfer into *Cx3cr1*^{Cre}*:Dicer* $^{fl/fl}$ recipients (*Cx3cr1*^{Cre}*:Dicer*$^{fl/fl}$*: RosaYfp* > *Cx3cr1*^{Cre}*:Dicer*$^{fl/fl}$).

Interestingly, both *Cx3cr1*^{Cre}*:Dicer*$^{fl/fl}$ recipient groups (WT>*Cx3cr1*^{Cre}*:Dicer*$^{fl/fl}$, and *Cx3cr1*^{Cre}*:Dicer*$^{fl/fl}$*:RosaYfp* > *Cx3cr1*^{Cre}*:Dicer*$^{fl/fl}$) developed motoric deficiencies indicated by reduced locomotor activity and an impaired ability to grip wire (**Fig. 11A, B**), therefore WT BM transfer did not result in a rescue of the motoric deficiency. Analysis of the chimerism of the brain macrophage compartment, revealed that the WT recipients mice (CD45.1^{+}) WT >WT and *Cx3cr1*^{Cre}*:Dicer*$^{fl/fl}$*: RosaYfp* >WT) showed 3% and 6% engraftment, respectively. Surprisingly and in stark contrast, the WT (CD45.1^{+}) >*Cx3cr1*^{Cre}*:Dicer*$^{fl/fl}$ group showed > 95% engraftment with donor-derived cells (**Fig. 11C-E**), indicating that *Dicer* deficiency turns the otherwise radio-resistant microglia into radio-sensitive, and accordingly they are ablated by lethal irradiation

and replaced with BM derived cells. This result was further established by histological analysis of L5-SC microglia in *Cx3cr1*^{Cre}*:Dicer*$^{fl/fl}$ recipients transferred with *Cx3cr1*^{Gfp} BM ((*Cx3cr1*^{Gfp} > *Cx3cr1*^{Cre}*:Dicer* $^{fl/fl}$) BM chimeras), showing that all Iba^{+} cells were also GFP^{+} (**Fig. 11F**). *Dicer* deficient microglia radio-sensitivity could be explained by the finding of a recent study showing that *Dicer* is required for a proper DNA damage response to irradiation [115]. Dicer-deficient microglia exposed to lethal irradiation might accumulate a high level of DNA damage directing them towards apoptosis. However, despite the complete replacement of the *Dicer*-deficient microglia by WT cells, no functional rescue of *Cx3cr1*^{Cre}*:Dicer* $^{fl/fl}$ recipients was achieved as the motoric deficiency persisted.

Interestingly, we also observed Mac2^{+} GFP^{+} cells accumulation in L5 ventral roots of *Cx3cr1*^{Cre}*:Dicer*$^{fl/fl}$ recipients transferred with *Cx3cr1*$^{Gfp+}$ BM ((*Cx3cr1*$^{Gfp+}$ > *Cx3cr1*^{Cre}*:Dicer* $^{fl/fl}$) BM chimeras) (**Fig. 11G, G'**), indicating that Mac2^{+} cells were partially monocyte-derived cells, in line with earlier reports [95, 96]. In contrast, Mac2^{+} cells did not accumulate in *Cx3cr1*^{Cre}*: Dicer* $^{fl/fl}$*: RosaYfp* >WT BM chimeras, (**Fig. 11H, H'**), establishing that dicer deficient monocytes, derived from *Cx3cr1*^{Cre}*: Dicer* $^{fl/fl}$*: RosaYfp* BM do not give rise to L5 motor root Mac2^{+} cells in absence of a pre-existing neurological disorder in recipient mice.

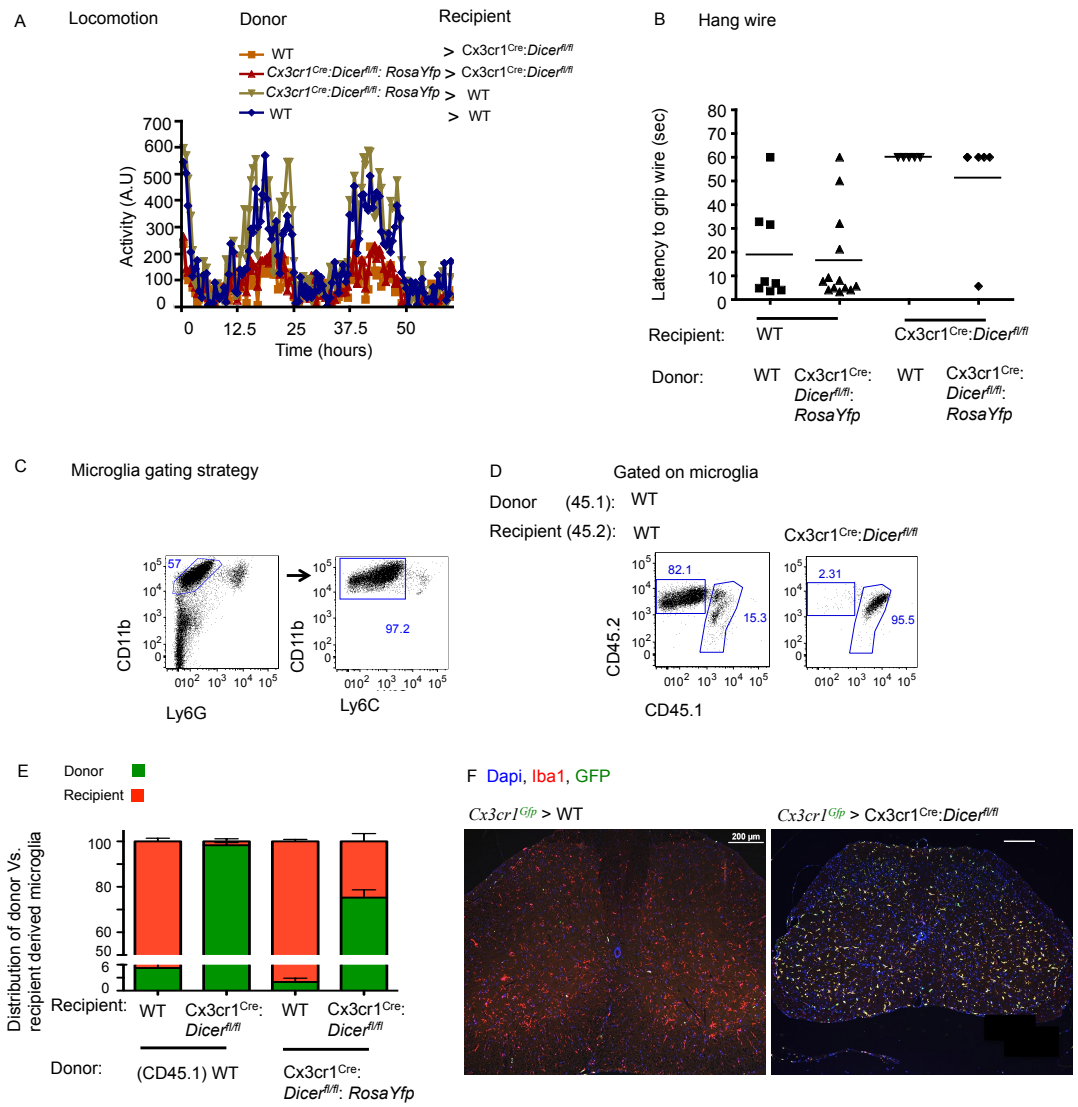

Figure 11 (A-F). Cx3cr1^{Cre}:Dicer$^{fl//fl}$ Vs. Dicer$^{fl/fl}$ mice motoric disorder is not rescued by a WT BM transfer. (A) A graphical summary showing home-cage locomotion during continuous periods of light (X-axis, marked in yellow) and dark (X-axis, marked in gray), revealing that *Cx3cr1^{Cre}:Dicer$^{fl//fl}$* recipient mice have reduced activity during dark period regardless of the transferred BM (CD45.1^{+} (WT), or *Cx3cr1^{Cre}:Dicer$^{fl//fl}$*). *Cx3cr1^{Cre}:Dicer$^{fl//fl}$* BM transfer into WT recipients did not affect this motoric function. (B) A graphical summary showing hang wire test, revealing that *Cx3cr1^{Cre}:Dicer$^{fl//fl}$* recipient mice have reduced ability to grip wire regardless of the transferred BM (WT or *Cx3cr1^{Cre}:Dicer$^{fl//fl}$*). *Cx3cr1^{Cre}:Dicer$^{fl//fl}$* BM transfer into WT recipients did not affect this motoric function. (C) A flow cytometry gating strategy of SC microglia recognized as CD11b^{+}Ly6C^{-}Ly6G^{-}. (D) Representative flow cytometry dot plots of SC microglia from CD45.1^{+} WT into CD45.2^{+} WT or CD45.2^{+}: *Cx3cr1^{Cre}:Dicer$^{fl//fl}$* recipients, showing distribution of microglia population between donor and recipient derived cells. (E) A graphical summary of the relative contribution of donor versus recipient derived cells to the SC microglia pool, in CD45.1^{+} WT BM transfer into CD45.2^{+} WT or CD45.2^{+}:*Cx3cr1^{Cre}:Dicer$^{fl//fl}$* recipients, according to CD45.1 expression, and in *Cx3cr1^{Cre}:Dicer$^{fl//fl}$:RosaYfp* BM transfer into WT or *Cx3cr1^{Cre}:Dicer$^{fl//fl}$* recipients, according to YFP expression. (F) Representative immunofluorescent images of SC-L5 area from *Cx3cr1^{Gfp}* into WT and *Cx3cr1^{Gfp}* into *Cx3cr1^{Cre}:Dicer$^{fl//fl}$* chimeric mice, showing staining for microglial marker Iba1 (red), donor derived marker CX$_3$CR1-GFP (green), and nuclei counterstaining-Dapi (blue). *Cx3cr1^{Gfp}* into *Cx3cr1^{Cre}:Dicer$^{fl//fl}$* mice show that all Iba1^{+} cells are donor derived (GFP^{+}).

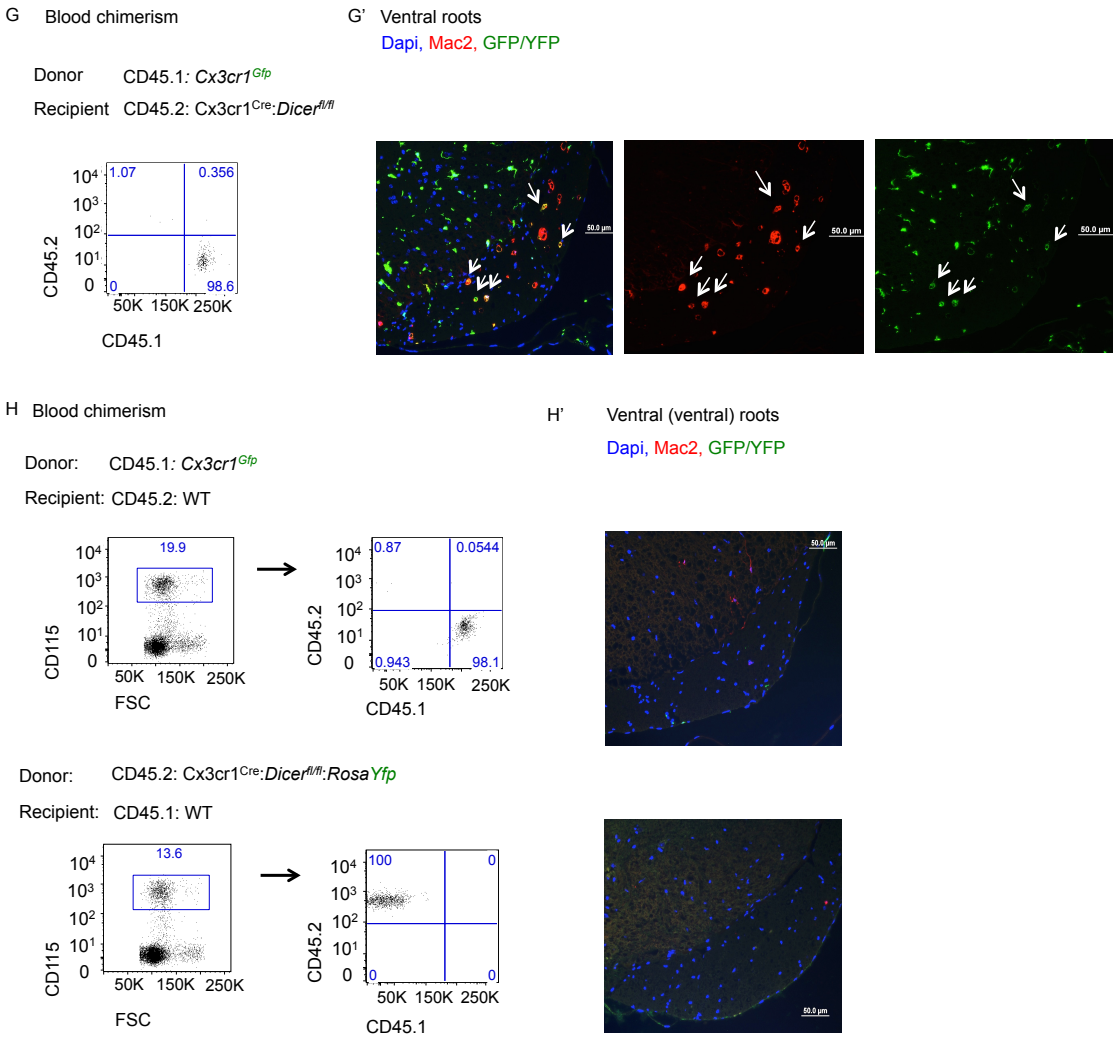

Figure 11 (G,H). L5 accumulated Mac2$^+$ cells are partially monocyte derived. (G) CD45.1: *Cx3cr1^{Gfp}* into CD45.2: *Cx3cr1^{Cre}:Dicer$^{fl//fl}$* chimeric mice showing complete (90-100% donor) chimerism according to representative flow cytometry dot plots of blood monocytes. (G') *Cx3cr1^{Gfp}* into *Cx3cr1^{Cre}:Dicer$^{fl//fl}$* chimeric mice revealing an infiltration of Mac2$^+$GFP$^+$ (white arrows) cells according to representative immunoflourescent images of motoric roots showing staining for Mac2 (red) CX_3CR1-GFP (green) and nuclei counterstaining-Dapi (blue). (H) CD45.1:*Cx3cr1^{Gfp}* into CD45.2: WT, and CD45.2: *Cx3cr1^{Cre}:Dicer$^{fl//fl}$ -RosaYfp* into CD45.1: WT chimeric mice showing complete (90-100% donor) chimerism according to representative flow cytometry dot plots of blood monocytes. (H') *Cx3cr1^{Gfp}* into WT, and *Cx3cr1^{Cre}:Dicer$^{fl//fl}$ -RosaYfp* into WT chimeric mice revealing no infiltration of Mac2$^+$ cells according to representative immunoflourescent images of motoric roots showing staining for Mac2 (red), CX_3CR1-GFP/YFP (green) and nuclei counterstaining-Dapi (blue). Graphical data are expressed as mean +/- SEM, n=4 in each group of chimeric mice. Statistical testing was performed with students T test. (* P<0.05, ** P<0.01).

2.10 *Cx3cr1*^{Cre}*:Dicer* $^{fl/fl}$ mice show a depletion of skin resident cells including Langerhans cells (LC) and dendritic epidermal T cells (DETCs).

The skin harbors two populations of tissue-resident cells targeted in the *Cx3cr1*^{Cre} mouse, Langerhans cells (LC) and CX_3CR1-expressing γδT cells, also referred to as "dendritic epidermal T cells (DETCs)" [116, 117]. LC are a unique subset of epidermal dendritic cells that carry features of macrophages, and are like other resident macrophages, generated during embryonic development from CX_3CR1^+ precursors. LC are hence targeted in the *Cx3cr1*^{Cre} mouse [80]. Using *CD11c*^{Cre}*:Dicer*$^{fl/fl}$ mice, it has been reported that *Dicer*-deficient LC undergo apoptosis [98]. Interestingly, populations of both LC and γδT cells were found significantly reduced in *Cx3cr1*^{Cre}*:Dicer* $^{fl/fl}$ mice, indicating that - in stark contrast to the microglia - *Dicer* and presumably miRs are essential to maintain not only LC, but also other long-lived epidermal tissue resident cells **(Fig. 12A, B)**.

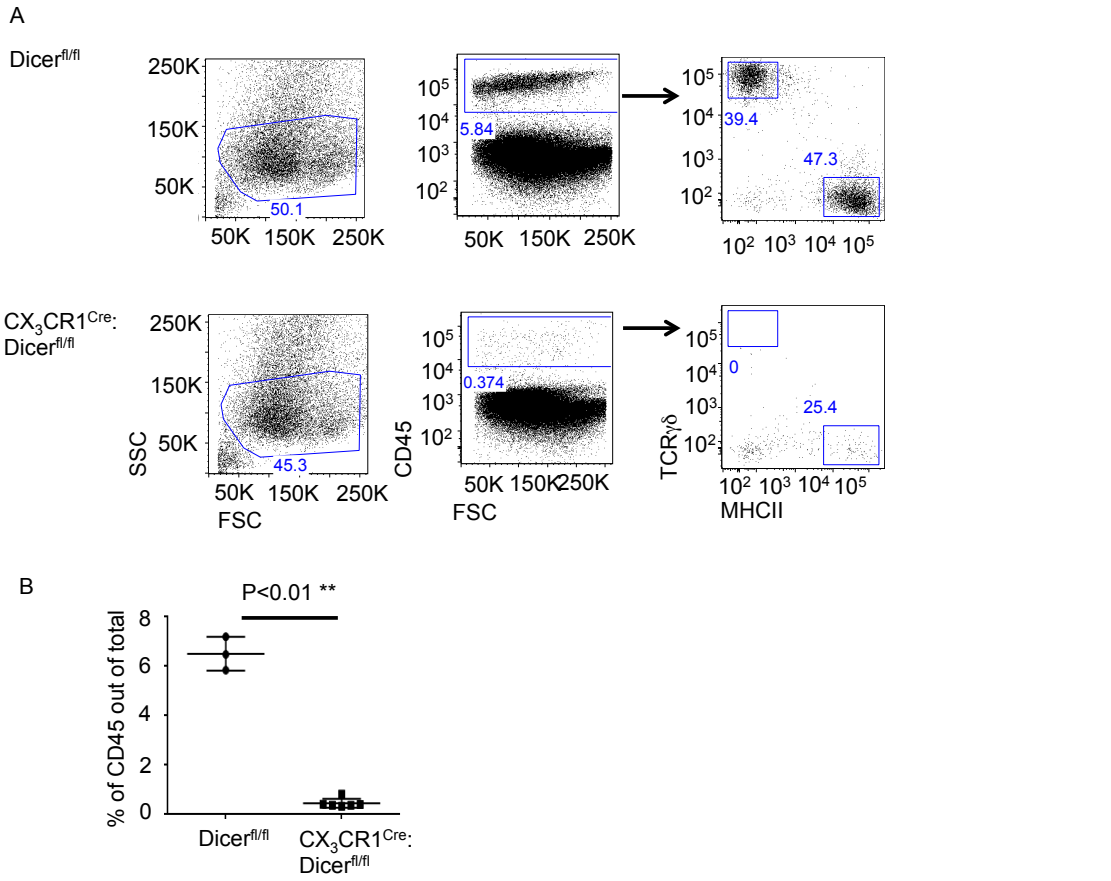

Figure 12. Cx3cr1*^{Cre}*:Dicer*$^{fl/fl}$ *mice show a depletion of epidermal resident cells. (A) Representative flow-cytometry dot plot analysis for epidermal $CD45^+$ cells, including LC $CD45^+MHCII^+$ and γδT cells $CD45^+TCR\gamma\delta^+$. (B) Graphical summary showing a substantial reduction in *Cx3cr1*^{Cre}*:Dicer*$^{fl/fl}$ epidermal $CD45^+$ cells, consisting mainly out of LC and γδT cells. Graphical data are expressed as mean +/- SEM; n=3 of *Dicer*$^{fl/fl}$, and n=6 of *Cx3cr1*^{Cre}*:Dicer*$^{fl/fl}$ mice. Statistical testing was performed with students T test. (* P<0.05, ** P<0.01).

2.11 Post-natal induction of *Dicer* loss in microglia, utilizing *Cx3cr1*^{CreER}*:Dicer*$^{fl/-}$ mouse model.

Cx3cr1^{CreER}*:Dicer*$^{fl/-}$ microglia are targeted already during embryonic development, since they are derived from CX_3CR1^+ yolk sac precursors that seed the developing CNS as early as E9.5. We wanted to test, if we would observe a similar phenotype when the mutation is induced after birth. For this end, we postnatally induced a microglia-specific *Dicer* loss by tamoxifen treatment of *Cx3cr1*^{CreER}*:Dicer*$^{fl/-}$ mice, resulting in a nuclear translocation of the Cre recombinase and ensuing rearrangements [80]. Moreover, *Cx3cr1*^{CreER}*:Dicer*$^{fl/-}$ mice allow a more specific genetic targeting of microglia vs. other macrophages, since tamoxifen is given postnataly, when most tissue-resident macrophages, except for microglia and intestinal macrophages stop to express CX_3CR1 [80]. Furthermore, intestinal macrophages are constantly replenished by blood monocytes [118], and therefore progressively lose the rearranged alleles [79, 119]. In contrast, microglia are long-lived, self-maintain and hence remain modified [79, 119]

2.11.1 *Cx3cr1*^{CreER}*:Dicer*$^{fl/-}$ *mice show an efficient Dicer loss in microglia.*

To increase the efficiency of complete *Dicer* gene deletion, we generated *Cx3cr1*^{CreER}*:Dicer*$^{fl/-}$ mice, that harbor one mutant and one 'floxed' (fl) *dicer* allele [90]. Of note, heterozygote *Dicer* mutant mice are viable and have no overt phenotype [120]. *Cx3cr1*^{CreER}*:Dicer*$^{fl/-}$ mice were treated with tamoxifen during the first week after birth (3 injections) and an additional dose was given at P30 (2 injections) to increase deletion efficiency, mice were analyzed at the age of 3 months **(Fig. 13A).** To validate the *Dicer* deletion in microglia, the cells were sorted using flowcytometry (**Fig. 13B**). PCR analysis for genomic DNA confirmed that *Cx3cr1*^{CreER}*:Dicer*$^{fl/-}$ mice had lost the 'floxed' dicer allele (**Fig. 13C**). Quantitative RT-PCR analysis revealed a ~50-100 fold reduction in miR146a and miR142-3p expression and a 5-10 fold reduction in miR200c expression in microglia isolated from tamoxifen-treated *Cx3cr1*^{CreER}*:Dicer*$^{fl/-}$ mice (**Fig. 13D**).

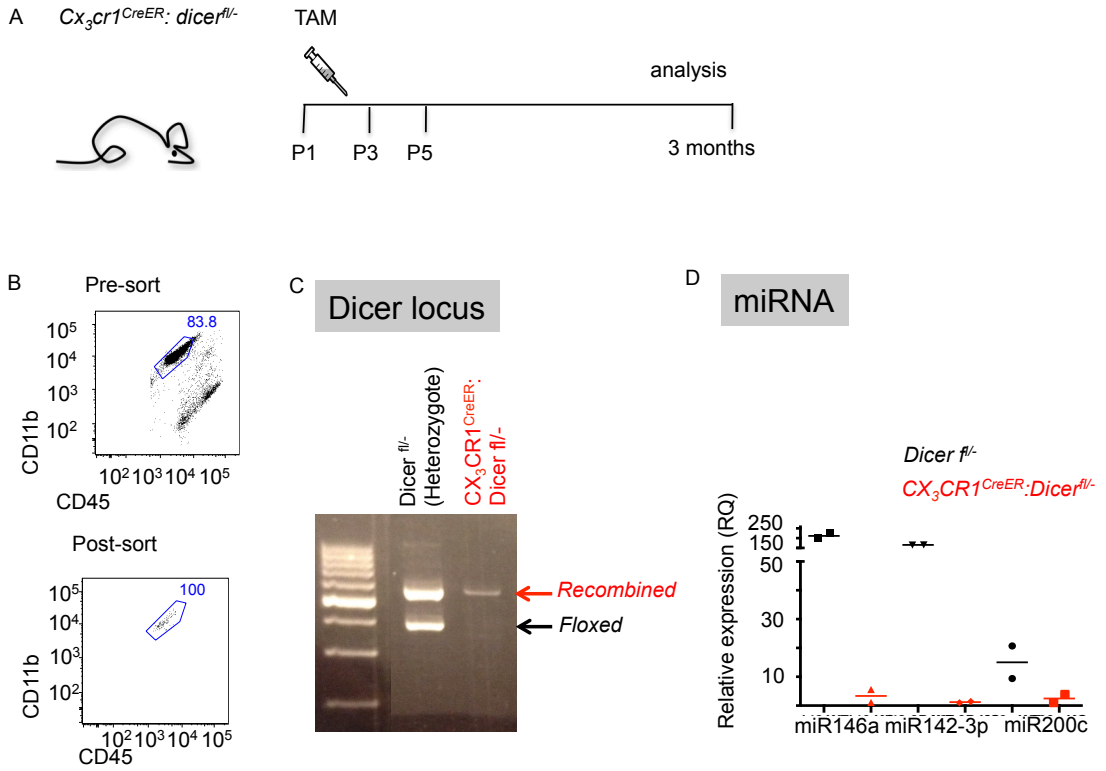

Figure 13. Cx3cr1^{CreER}:Dicer$^{fl/-}$ mice show an efficient Dicer loss in microglia.
(A) A scheme describing the transgenic mouse model used for microglia induced *Dicer* deletion. (B) Flow cytometry analysis images showing sorted brain microglia from either *Cx3cr1^{CreER}:Dicer$^{fl/-}$* or *Dicer$^{fl/-}$* mice pool (n=6 for each pool). Microglia were characterized as Ly6G^{neg}Ly6C^{neg}CD45^{int}CD11b^{+} cells. (C) A Representative genomic PCR analysis image showing the PCR product for *Dicer* exon 24 deleted allele. *Cx3cr1^{CreER}:Dicer$^{fl/-}$* mice show only recombined allel while *Dicer$^{fl/-}$* mice had both recombined and "fl" allel. (D) Graphical summary showing qRT-PCR analysis for miR-146a, miR-142-3p and miR-200c expression within Microglia sorted from brains of *Cx3cr1^{CreER}:Dicer$^{fl/-}$* or *Dicer$^{fl/-}$* mice. Data are expressed as mean +/- SEM, statistically analyzed with student T test (n=2 per group).

2.11.2 Unchallenged *Cx3cr1^{CreER}:Dicer$^{fl/-}$* mice display no overt phenotype.

Following the validation of the *Dicer* deletion, we analyzed the *Cx3cr1^{CreER}:Dicer$^{fl/-}$* mice for signs of motoric dysfunction, astrocytosis and microglia activation. Motoric activity was examined three months following tamoxifen treatment and histological assessments for astrocytosis, and microglia activation were performed six months following tamoxifen treatment. Hang wire test analysis for hind leg motility of *Cx3cr1^{CreER}: Dicer$^{fl/-}$* mice revealed no motoric impairment **(Fig. 14A)**, in line with the absence of astrocytosis in the SC-L5 area **(Fig. 14B)**. Microglia of tamoxifen-treated *Cx3cr1^{CreER}:Dicer $^{fl/-}$* mice also showed no signs of activation **(Fig. 14C)**. Overall, the postnatal induction of microglial dicer deficiency did not result in an overt phenotype. This is in stark contrast to the microglia of *Cx3cr1^{Cre}:Dicer$^{fl/fl}$* mice, which display a spontaneous, though delayed development of motor dysfunction, associated with prominent microglia activation.

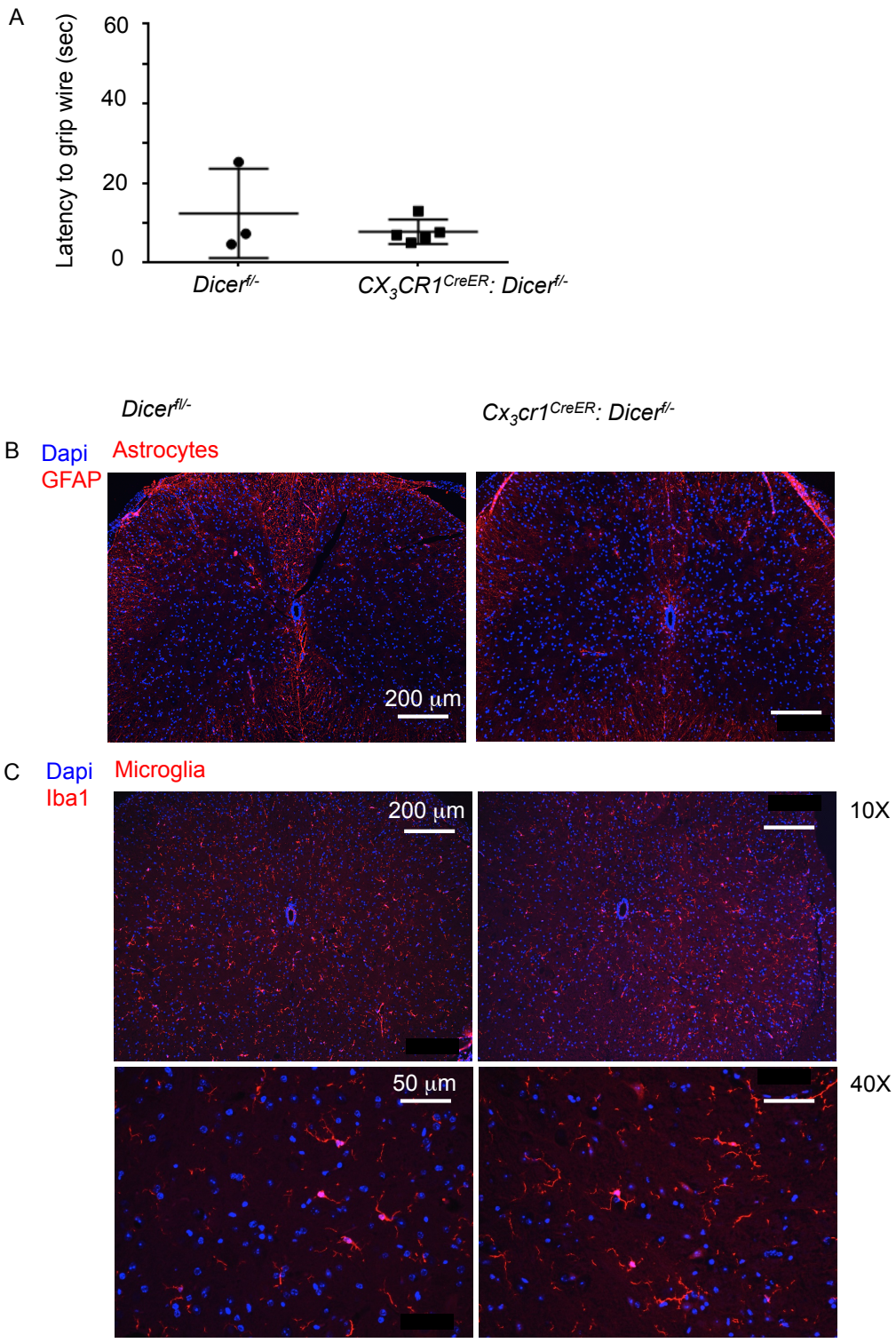

Figure 14. **Unchallenged *Cx3cr1*^{CreER}*:Dicer*$^{fl/-}$ mice display no overt phenotype.**
(A) A graphical summary of hang-wire test showing there is no significant difference between *Dicer*$^{fl/-}$ *and Cx3cr1*^{CreER}*:Dicer*$^{fl//-}$ in latency to grip wire. Data are displayed as mean +/- SEM, and statistically analyzed with students T test (n=3 and n=5 for *Dicer*$^{fl/-}$ and *Cx3cr1*^{CreER}*: Dicer*$^{fl/-}$ mice, respectively). (B) Representative fluorescent microscopic images of paraffin sections of SC-L5 segment extracted from *Dicer*$^{fl/-}$ or *Cx3cr1*^{CreER}*:Dicer*$^{fl/-}$ mice showing staining for GFAP (red) and Dapi (blue). (C) A representative fluorescent microscopic images of paraffin sections of SC-L5 segment extracted from *Dicer*$^{fl/-}$ or *Cx3cr1*^{CreER}*:Dicer*$^{fl/-}$ mice showing staining for Iba1 (red) and Dapi (blue).

2.11.3 Microglia of *Cx3cr1^{CreER}:Dicer $^{fl/-}$* mice are radio-sensitive.

Cx3cr1^{Cre}:Dicer$^{fl/fl}$ microglia are radio-sensitive, as indicated by their quantitative replacement by BM-derived cells in chimeras (**Fig 11**). To examine the radiosensitivity of microglia that was postnatally depleted of the *Dicer* gene, we lethally irradiated *Dicer$^{fl/-}$* (WT) and *Cx3cr1^{CreER}:Dicer$^{fl/-}$:RosaYfp* mice (both CD45.2) and engrafted them with CD45.1^{+} *Cx3cr1^{Gfp+}* BM. Microglia of *Cx3cr1^{CreER}:Dicer$^{fl/-}$:RosaYfp* mice are CD45.2^{+} and following exposure to tamoxifen will become YFP^{+} **(Fig. 15A),** while microglia of WT recipients will be only CD45.2^{+}. In order to examine the chimerism of the resulting mice, we measured contribution of donor and recipient cells to the blood monocyte compartment. The analysis revealed a complete hematopoietic reconstitution by donor cells in both *Dicer$^{fl/-}$* and *Cx3cr1^{CreER}:Dicer$^{fl/-}$:RosaYfp* recipients **(Fig. 15B).** The analysis of microglia population chimerism showed that 40% of the *Cx3cr1^{CreER}:Dicer$^{fl/-}$:RosaYfp* microglia were substituted by BM-derived CD45.1^{+}CX$_3$CR1^{GFP+} cells in comparison with <2% substitution in *Dicer$^{fl/-}$* recipients **(Fig. 15C, D)**. Of note, the remaining 60% endogenous microglia of *Cx3cr1^{CreER}:Dicer$^{fl/-}$:RosaYfp* mice were YFP^{+}, indicating that they had recombined the *Rosa-Stop-Yfp* allele only, but not the *Dicer* allele. The animals had been treated with a high dose of tamoxifen to induce efficient recombination in microglia. However, rare cells bearing a single recombination of the *Stop-Yfp* (YFP^{+} only) might have an advantage over the *Dicer* deleted cells (YFP^{+}Dicer^{null}) and since microglia are dividing cells, might out-compete the *Dicer* deleted cells with time. Of note, in this experiment BM transplantation was performed 6 months post tamoxifen treatment, allowing for a progessive replacement of *Dicer*-deficient cells.

Taken together, the above results show that postnatally *Dicer*-deleted microglia (*Cx3cr1^{CreER}:Dicer$^{fl/-}$*) are indeed *Dicer* deficient. However unlike embryonically *Dicer*--deleted microglia (*Cx3cr1^{Cre}:Dicer$^{fl/fl}$*), this didn't result in a microglial activation phenotype nor did it cause neuronal damage or a motoric phenotype.

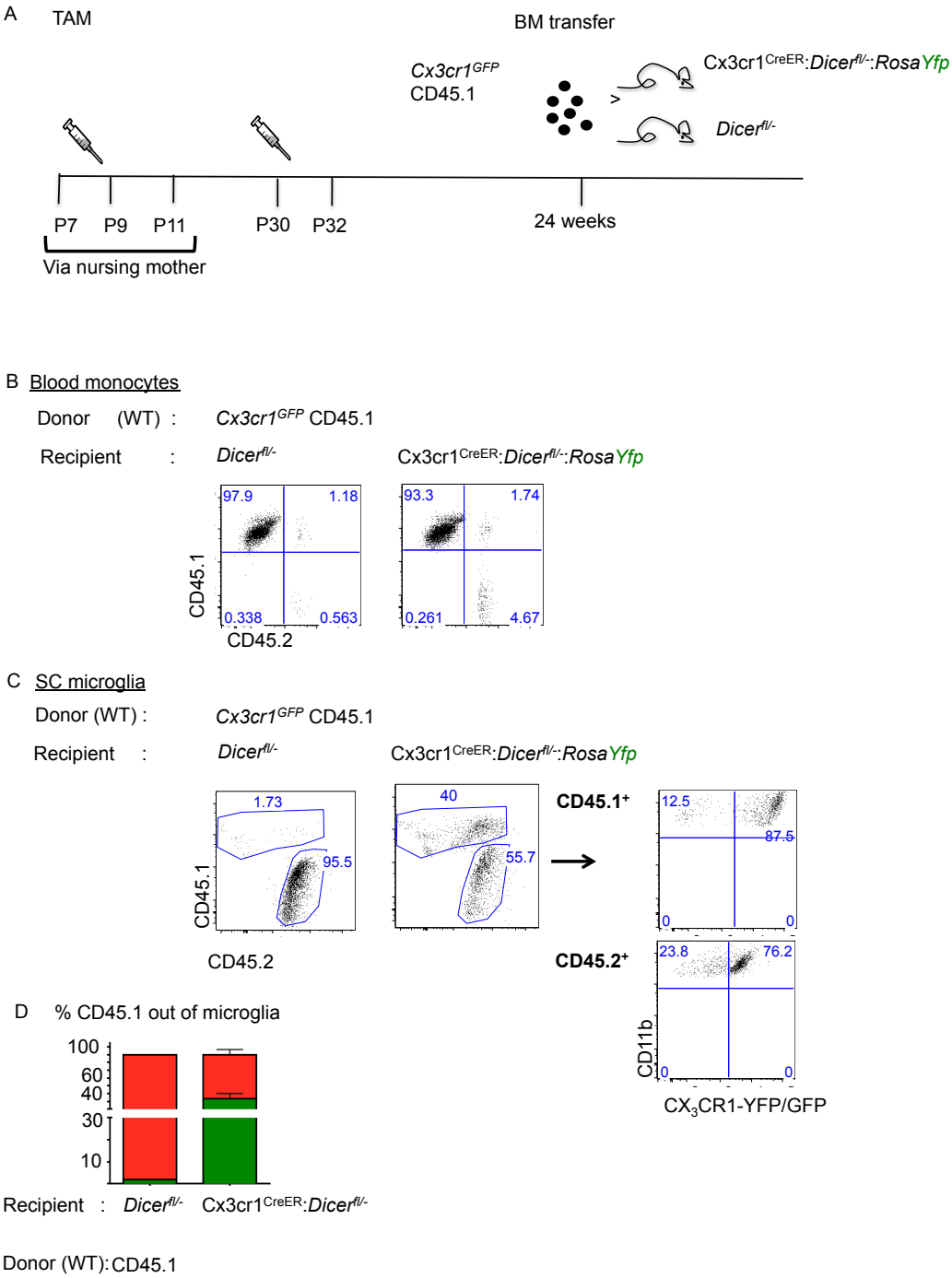

Figure 15. Cx3cr1^{CreER}:Dicer$^{fl/-}$-RosaYfp microglia are becoming radiosensitive and can be replaced by BM derived cells following lethal irradiation. (A) A time frame scheme describing tamoxifen treatment and chimerism of *Cx3cr1^{CreER}:Dicer$^{fl/-}$-RosaYfp* and *Dicer$^{fl/-}$* mice. (B) Representative flow cytometry dot plots showing distribution of Blood monocytes (CD115^{+}) between donor and recipient BM derived cells, in *Dicer$^{fl/-}$* or *Cx3cr1^{CreER}:Dicer$^{fl/-}$-RosaYfp* recipients transferred with CD45.1^{+}*Cx3cr1^{Gfp}*(WT) BM. (C) Representative flow cytometry dot plots showing distribution of SC microglia (CD11b^{+}Ly6C^{+}Ly6G^{+}), between donor's and recipient's origin. Donor microglia are CD45.1^{+}*Cx3cr1^{Gfp}* while endogenous Microglia are either CD45-2^{+} only or CD45-2^{+}YFP^{+} in tamoxifen treated *Dicer$^{fl/-}$* or *Cx3cr1^{CreER}:Dicer$^{fl/-}$-RosaYfp* recipients, respectively. (D) Graphical summary of the SC microglia distribution between donor and recipient derived cells, according to the CD45.1 marker expression. (n=2 for each group) Graphical data are expressed as mean +/- SEM, Statistical testing was performed with students T test. (* P<0.05, ** P<0.01).

3. Materials and Methods.

Mice. The following 4 - to 24-week-old mice were used**:** C57BL/6 (CD45.2); CD45.1 mice (B6.SJL-*Ptprca Pep3b*/Boyj, Jackson Laboratories) bearing the CD45.1 allotype; *Cx3cr1*$^{gfp/+}$ mice (B6.129P-Cx3cr1tm1Litt/J, Jackson Laboratories) harboring a targeted replacement of the *Cx3cr1* gene by an enhanced GFP reporter gene [81]; *Cx3cr1*^{Cre} mice harboring a targeted replacement of the *Cx3cr1* gene by a Cre recombinase [80] generated on a C57Bl/6 background; *Cx3cr1*^{CreER} mice harboring a targeted replacement of the *Cx3cr1* gene by a Cre recombinase fused to a mutant estrogen ligand-binding domain [80], requiring the presence of the estrogen antagonist tamoxifen (TAM) for activation; *Pgk*^{Cre} mice ("ubiquitous Cre mice") (B6.C-Tg(Pgk1-cre)1Lni/CrsJ, Jackson laboratories) harboring Cre recombinase under the control of phosphoglycerate kinase 1 (*Pgk1*) promoter [121], activate in all mouse tissues; *Dicer*$^{fl/fl}$ mice (B6.Cg-*Dicer1tm1Bdh*/J, Jackson laboratories) harboring *loxP* sites on either side of exon 24 of the targeted gene [90]; and Rosa-26-YFP mice (B6.129X1-*Gt(ROSA)26Sortm1(EYFP)Cos*/J, Jackson laboratories) harboring Enhanced Yellow fluorescent protein gene (EYFP) inserted into the *Gt(ROSA)26Sor* locus blocked by an upstream *loxP*-flanked STOP sequence [122]. *Cx3cr1*^{Cre} mice were crossed with *Dicer*$^{fl/fl}$ mice, generating *Cx3cr1*^{Cre}: *Dicer*$^{fl/fl}$. *Cx3cr1*^{Cre}: *Dicer*$^{fl/fl}$ mice were crossed with *RosaYfp* mice, generating *Cx3cr1*^{Cre}*: Dicer*$^{fl/fl}$ *–RosaYfp* mice. *Pgk*^{Cre} mice were crossed with *Dicer*$^{fl/fl}$ mice, generating *Dicer*$^{WT/-}$. *Cx3cr1*^{CreER} mice were crossed with *Dicer*$^{fl/-}$ mice, generating *Cx3cr1*^{CreER}: *Dicer*$^{fl/-}$. *Cx3cr1*^{CreER}: *Dicer*$^{fl/-}$ mice were crossed with *RosaYfp* mice, generating *Cx3cr1*^{CreER}: *Dicer*$^{fl/-}$- *RosaYfp* mice. *Cx3cr1*$^{gfp/+}$ mice were crossed with CD45.1 mice, generating CD45.1:*Cx3cr1*$^{gfp/+}$.

For *Cx3cr1*$^{\underline{Cre}}$: *Dicer*$^{fl/fl}$ microglia replacement experiment, the following BM chimeras were generated: [CD45.1:*Cx3cr1*$^{gfp/+}$> wt], [CD45.1:*Cx3cr1*$^{gfp/+}$> *Cx3cr1*^{Cre}*: Dicer*$^{fl/fl}$], [*Cx3cr1*^{Cre}*: Dicer*$^{fl/fl}$ *–RosaYfp*> CD45.1], [*Cx3cr1*^{Cre}*: Dicer*$^{fl/fl}$ *–RosaYfp* > *Cx3cr1*^{Cre}*: Dicer*$^{fl/fl}$].

For *Cx3cr1*$^{\underline{CreER}}$: *Dicer*$^{fl/-}$ microglia replacement experiment, The following BM chimeras were generated: [CD45.1:*Cx3cr1*$^{gfp/+}$> *Dicer*$^{fl/-}$], [CD45.1:*Cx3cr1*$^{gfp/+}$> *Cx3cr1*^{CreER}: *Dicer*$^{fl/-}$*–RosaYfp*].

BM chimera animals were lethally irradiated (950 rad) and reconstituted the following day via *i.v* injection of donor whole BM cells, 5X10^6 cells were injected per mouse. All animals were maintained in specific pathogen-free (SPF) conditions and handled

according to protocols approved by the Weizmann Institute Animal Care Committee as per international guidelines.

Cell isolation, flow cytometry and sorting of microglia, colonic macrophages, liver macropahges, and epidermal resident cells.

Cell isolation and labeling. Microglia isolation was performed as follows: mice were anesthetized with thio-pental (100 mg/kg) and perfused with PBS. Whole brain and SC were exiced, homogenized, and incubated with HBSS containing 2% BSA, 1mg/ml Collagenase D (Roche), and 0.1 mg/ml DNaseI (Roche) at 37^{O}C. Next, the cell homogenate was filtered through a 70 micron strainer (BD Biosciences), and centrifuged on a 40% percoll (Sigma) gradient, 1000 rcf, no acceleration and brakes, at room temperature. Pellet containing microglia (mononuclear cells enriched with microglia) was washed and subsequently stained for flow cytometry analysis.

*PBS and HBSS solutions were without Ca^{2+} and Mg^{2+}. Microglia labeling strategy was $Ly6C^{-}Ly6G^{-}CD45^{+}CD11b^{+}$.

Epidermal LC and gdT cells isolation was performed as follows: ears were excised and gently separated into two layers placed on trypsin C medium (Beit Haemek industries) with epidermis facing liquid, at 37^{0}C for 50 min. Epidermis was then carefully removed, meshed through a 70 micron cell strainer and washed with PBS. LC labeling strategy was $CD45^{+}I\text{-}Ab^{+}$, γδT cells labeling strategy was $CD45^{+}TCR\gamma\delta^{+}$.

Colonic macrophage were isolated as published before [123]; accordingly, labeling strategy was $Ly6C^{-}CD45^{+}I\text{-}Ab^{+}CD11b^{+}CD64^{+}$.

Liver macrophages were isolated as published before [124]; accordingly, labeling strategy was $Ly6C^{-}CD45^{+}I\text{-}Ab^{+}CD11b^{+}F4/80^{+}CD64^{+}$.

Antibodies. CD45 (clone: 30F11), CD11b (clone: M1/70), Ly6C (clone: HK1.4), Ly6G (clone: 1A8), CD86 (clone: GL-1), I-Ab (clone: AF6-120.1), CD68 (clone: FA-11), TCRgd (clone: GL3), CD115 (clone: AFS98), F4/80 (clone: CI:A3-1), CD64 (clone: X54-5/7.1). Cells were analyzed with a LSRFortessa flow cytometer (BD) or sorted with a FACSAria machine (BD). Flow cytometry anal- ysis was done with the FlowJo software.

Microarray analysis.

Affymetrix mRNA analysis. Total RNA was extracted from microglia freshly isolated from $CX3CR1^{Cre}$: $Dicer^{fl/fl}$, $Dicer^{fl/fl}$ mice. RNA extraction was performed with the miRNeasy Mini or Micro Kit (Qiagen). RNA quantity, purity and integrity was

assessed with ND-1000 Nanodrop (Peqlab) and BioAnalyzer 2100 (Agilent). The cDNA was prepared, labeled and hybridized to Affymetrix GeneChip, mouse gene 1.0 ST according to standard manufacturer protocols. Hybridized chips were stained and washed and were scanned using the Affymetrix GeneChip 3000 7G plus scanner. Affymetrix GeneChip Operating Software (GCOS v1.4, http://www.affymetrix.com) was used for the initial analysis of the microarray data to convert the image files to cell intensity files (CEL). Transcriptome analysis was carried out using Partek Genomic Suite 6.6 (Inc. St. Charles, MO; www.partek.com). The raw probe intensities were adjusted based on the number of G and C bases in the probe sequence, before any probe correction. Preprocessing was preformed using the Robust Microarray Averaging algorithm (Irizarry et al., 2003). Genes expressed below background in all examined conditions were removed from further analysis. Statistical analysis was performed with anova. Differentially expressed genes were defined as those having fold change above or below 2 and p-value<0.05.

Agilent miR analysis.

Total RNA from WT microglia, colonic macrophages, and liver macrophages freshly isolated cells was extracted using the miRNeasy Mini Kit (QIAGEN) including DNase digest (QIAGEN). RNA purity was assessed with a BioAnalyzer 2100 (Agilent Technologies). Expression levels of miRNAs were assayed by Agilent miRNA microarrays (Release 12.0 and 15.0), according to the manufacturer's protocols. Then, 100 ng of total RNA per sample (duplicates for each cell population from independent sorts) was labeled and hybridized according to the manufacturer's instructions. For K-Means clustering with Pearson correlation, only miRNAs with a ≥ 2-fold differential expression in at least 1 population were used. As a target prediction algorithm, TargetScan 6.2 [125] was applied. For mRNA microarray analysis, total RNA was extracted and subjected to gene-expression profiling using the Mouse Genome Gene 1.0 ST Affymetrix Exon Microarray according to the manufacturer's instructions. For RNA sequencing (RNA-Seq) and ChIP followed by massive parallel sequencing (ChIP-Seq), total RNA was extracted with QIAzol reagent following the miRNeasy kit's procedure (QIAGEN), and sample quality was tested on a 2100 Bioanalyzer (Agilent). RNA-A+-Seq libraries were prepared using the ′dUTP second-strand (strand-specific) protocol. For detailed information, see the Methods section in [126].

qRT-PCR assay. miRNA expression quantification was performed on sorted microglia isolated from brain and SC of *CX3CR1*^{Cre}*: Dicer*$^{fl/fl}$, *Dicer*$^{fl/fl}$, *CX3CR1*^{Cre}*: Dicer*$^{fl/-}$, and *Dicer*$^{fl/-}$ mice. 50-250 ng of total RNA isolated with miRNeasy micro-kit (Qiagen) were reverse transcribed with the miScript reverse transcription kit (QIAGEN) according to the manufacturer's instructions. The miScript SYBR Green kit (QIAGEN) was used to detect amplification in a LightCycler 480 (Roche) machine. The following primers were used in combination with the universal primer (QIAGEN): U6, 5′-GATGACACGCAAATTCGTGAA-3′; miR-146a-5p, 5'-TGAGAACTGAATTCCATGGGT-3'; miR-142-3p, 5′-TGTAGTGTTTCCTACTTTATGGA-3′; miR-200c, 5'-TAATACTGCCGGGTAATGATGGA.

Significance was calculated with Students's *t*-test. All error bars in diagrams and numbers following a ± sign are standard deviations (s.d.).

Behavioral examination.

Home-cage locomotion. mice were single-housed, and locomotive activity was examined automatically over a 48-h period using the InfraMot system (TSE Systems, GmbH). ***Rotarod test*** mice were placed on an accelerating spinning wheel and their latency to fall was measured by an inframot beam. Mice were placed on a spinning wheel for five consecutive times, first two repetitions were considered training and last three repetitions were scored and averaged. ***Hangwire test*** mice were attached to a wire by their forelimbs and their latency to grip wire with hindlimbs was measured. Scoring equals the latency time, no grip or alternatively a fall was considered as "60 sec". Test was repeated 3 times with a 30 min gap between repetetions, scoring represented the average score of the three repetetions.

Histology. Mice were deeply anesthetized with thio-pental (100 mg/kg, administered i.p.) and transcardially perfused with 10 ml of PBS, followed by 100 ml of 2.5% (wt/ vol) paraformaldehyde (PFA) and left for 16-24hr in 2.5% PFA.

SC ChAT staining. Following PFA incubation, SC samples were equilibrated with a 30% (wt/ vol) sucrose for 48 hr, frozen with O.C.T (Tissue-Tek), and the entire L5 segment was sectioned with a microtom (Leica) into 30 μm thich sections. Every fifth section was labeled with ChAT (Chemicon, AB144P, 1:100) and Dapi, and labeled cells were counted (both ventral horns) and presented as the mean number of MNs per ventral horn.

SC Iba1and CD68. Following PFA incubation, SC was equilibrated with 30% (wt/ vol) sucrose solution for 48 hr. Next, samples were snap frozen in O.C.T (Tissue-Tek) by isopentane (sigma) previously cooled with liquid nitrogen, and sectioned with cryostat into 12 μm thick sections. Sections were stained with Iba1 (Wako, 019-19741, 1:150), CD68 (Biolegend, FA-11, 1:100) and Dapi. Labeled cells were counted (both ventral horns) and presented as the mean number of MNs per ventral horn.

SC Iba1and tunnel/ Ki67, SC Iba1 and anti GFP. Following PFA incubation, SC was embedded with paraffin, serially sectioned, antigen retrieved and stained. Antigen retrieval was performed with a sodium citrate PH 6 buffer in a pressure cooker. 6 μm Sections were stained with Iba1 (Wako, 1:150), Ki67 (Dako, TEC3, 1:100), TUNEL (TUNEL Kit from promega, according to the instruction manual), anti-GFP (Abcam, ab290, 1:100).

SC and brain GFAP. Following PFA incubation, SC was embedded with paraffin, serially sectioned, antigen retrieved and stained. Antigen retrieval was performed with a sodium citrate PH 6 buffer in a pressure cooker. 6 μm Sections were stained with GFAP (Dako, Z033429 1:200).

Ventral root L5 ChAT and Mac2. Following PFA incubation, L5 roots (motor and sensory) were excised embedded with paraffin, serially sectioned, antigen retrieved and stained. Antigen retrieval was performed with a sodium citrate PH 6 buffer in a pressure cooker. 2 μm Sections were stained with ChAT (Dako, Z033429 1:100), and Mac2 (M3/38, Cedarlane, 1:250).

Tamoxifen treatment.

To induce gene recombination in *Cx3cr1*^{CreER}*: Dicer*$^{fl/-}$ mice, tamoxifen was dissolved in warm olive oil, administered orally via gavage (Kiermayer et al., 2007) three times at P7, P9, and P11 (via lactating mother), followed by additional two administrations at P30 and P32, each injection was 10mg in a concentration of 10mg/ 100 μl. Mice were examined at least 6 weeks following treatment.

4. Discussion

Microglia are the resident macrophages of the CNS. These cells were shown to play a central role in the regulation of neuronal survival and function during homeostasis on the one hand, while promoting inflammatory processes during neurodegenerative disease on the other [127]. Similar to other macrophages, microglia are plastic and their differentiation and activity is controlled by the context of their local milieu. Regulatory mechanisms dictating microglia function are largely unknown, although recent data suggest that TGFβ may play a central role in the establishment of the unique tissue-specific genetic signature of adult microglia [13]. Interestingly and relevant to the present work, TGFβ induces in cultured microglia also the expression of several small non-coding miRs, including miR-99a, miR-125b-5p, and miR-342-3p. Yet, miR involvement in the regulation of microglia homeostasis remains elusive. Rather miRs have been shown to promote pro-inflammatory activities of microglia during pathological settings [71, 75-77]. The complete miR expression profile and their role in regulation of microglia functions within their native CNS environment has not been explored, mainly due to the lack of suitable experimental tools allowing *in vivo* targeting of microglia.

In this study we performed a molecular profiling of miR expression in adult microglia and show that these cells acquire a unique miR signature in comparison with other tissue resident macrophages, including liver macrophages and colonic macrophages. Emerging evidence highlight that macrophages are subjected to a process of tissue specialization imprinted by local factors to form an integral functional component in their tissue of residence [*Lavin et al., Cell 2014, in press*]. The fact that distinct tissue macrophages establish specific miR signatures might imply that these regulatory non-coding RNA components are part of the macrophage tissue specialization. Among the miRs we found to be highly expressed in microglia are miR-103-3p and 107-3p, which are predicted to target the neurotoxic factor *Cybb* [12]. An additional miR associated with down-regulation of inflammatory response is miR-146a-5p, highly expressed on both microglia and colonic macrophages, as compared with liver macrophages. Interestingly, the expression of this miR is elevated in CNS pathologies and on microglia isolated from mSOD1 mice [58, 75], implying on a negative immune-regulatory feedback function. Among the miRs highly expressed in microglia, we also noted miR-181c, which was shown to down-regulate expression of

TNFa and nitric oxide (NO) in a microglia cell-line exposed to hypoxia (simulating stroke like conditions), resulting in reduced death of co-cultured neurons [76, 77, 128]. Together, this suggests that some of the miRs of the unique microglial microRNA-ome could be important for down-regulation of microglial inflammatory pathways in the context of neuronal tissue damage [70, 77]. In addition, it is possible that anti-inflammatory miRs are important to maintain the quiescent profile of microglia during steady state or mild damage conditions, in which they are required for continuous surveillance and local repair processes [7, 8]. Strikingly, the *Dicer* deficiency in the *Cx3cr1*^{Cre}*:Dicer*$^{fl/fl}$ but not *Cx3cr1*^{CreER}*:Dicer*$^{fl/-}$ mice resulted in a significant visible neuronal-based motoric dysfunction. In *Cx3cr1*^{Cre}*:Dicer*$^{fl/fl}$ animals, the mutation is likely introduced during microglial seeding of neuro-epithelium as early as E 9.5, since microglia precursors express CX_3CR1^+ and they give rise to adult microglia which persist through life [3]. In the *Cx3cr1*^{CreER}*:Dicer*$^{fl/-}$ model, however, the *Dicer* mutation is only introduced postnataly via administration of tamoxifen. Notably, microglia of *Cx3cr1*^{Cre}*:Dicer*$^{fl/fl}$ mice display an activated morphology characterized by increased cell body size and reduced dendrite length as well as increased turnover. *Cx3cr1*^{Cre}*:Dicer*$^{fl/fl}$ mice display a significant motoric dysfunction, albeit only around 8 weeks. Interestingly, a similar delay between the establishment of the mutation and disease onset has also been observed in cerebellar and spinal cord motor neuron specific *Dicer*-deficient mouse models [59, 129]. Further histological evaluation of 8 weeks old *Cx3cr1*^{Cre}*:Dicer*$^{fl/fl}$ mice revealed profound astrocytosis accompanied by a later substantial motor neurons damage as shown by a 40% reduction of motor neurons cell bodies number and a loss of motoric axons in SC-L5 ventral root at 24 weeks of age. In addition, the L5 motor roots of *Cx3cr1*^{Cre}*:Dicer*$^{fl/fl}$ mice was populated with $Mac2^+$ cells which most likely comprise phagocytizing Schwann cells and macrophages, both are known to accumulate in damaged axons and promote axon regeneration [95, 130]. This accumulation was obvious already before visible motoric symptoms at 6 weeks of age. A similar accumulation of macrophages in ventral root has been reported in mSOD1 mice before disease onset [93]. Collectively, these results highlight the fact that miR-deficiency in microglia during embryogenesis leads to the establishment of progressive motoric disorder accompanied by profound astrocytosis and an increase in neuronal death.

Notably, although other resident tissue macrophages are also targeted with *Dicer*-

deficiency during embryogenesis in *Cx3cr1*^{Cre}*:Dicer*$^{fl/fl}$ mice, post-mortem histological assessment of 24-weeks old mice did not reveal any significant pathological manifestations in vital peripheral organs examined, such as the liver, intestine, skin, kidney and lungs (data not shown). Rather, the only consistant spontaneous pathological finding of *Cx3cr1*^{Cre}*:Dicer*$^{fl/fl}$ mice with high penetrance occurs, although with delay in the CNS. We speculate that the pathology results from the fact that embryonic microglia are crucially involved in the normal development of neuronal circuits and that miRs play an important role in the regulation of their tissue-specific microglia activities.

The microarray analysis of adult microglia of *Cx3cr1*^{Cre}*:Dicer*$^{fl/fl}$ mice further confirmed the activated phenotype observed in the histological analysis. Especially interesting was the up-regulation of the neurotoxic pro-inflammatory oxidase Nox2 (*Cybb*), which is located on the cellular membrane of microglia and whose activation induces damage to the surrounding tissue, especially neurons [86, 97]. Expression of Nox2 in our model is in line with studies that show Nox2 up-regulation in microglia in the context of various neurodegenerative diseases such as PD [131], AD [132, 133] and ALS [12]. Other up-regulated genes included the inflammatory mediators *S100a8,* and *S100a9,* which were also expressed in microglia from post-mortem AD patient lesions [134, 135] and in human cerebral ischemia brain sections [103]. Osteopontin (*Spp1)* was also up regulated and may be both neurotoxic and neuroprotective as it was shown to contribute to disease progression in autoimmune encephalomyelitis [109], but was also shown to ameliorate neuronal damage in a model of spinal cord injury [110, 136]. Interestingly, Osteopontin is also increased in SC microglia isolated from mSOD1 animals [12]. Altogether, our results show a pro-inflammatory neurotoxic phenotype for *Cx3cr1*^{Cre}*:Dicer*$^{fl/fl}$ deficient microglia at the adult stage, which could possibly be the cause for the observed neuronal damage and subsequent motoric phenotype. However, since we did not observe signs for microglia activation in *Cx3cr1*^{CreER}*:Dicer*$^{fl/-}$, we consider it more likely that the pro-inflammatory neurotoxic phenotype is secondary to a neuronal damage already established during embryonic development. To substantiate this assumption, we will analyze the impact of the Dicer and miR deficiency on gene expression regulation in *Cx3cr1*^{Cre}*:Dicer*$^{fl/fl}$ microglia during late embryonic development and early postnatal stages.

Supporting the idea that miRs are required for microglia developmental and

homeostatic functions, our microarray analysis revealed that *Dicer*-deficient microglia down-regulated genes associated with neuronal development. These included *Nav2*, a retinoic acid inducible protein that promote axonal guidance [111] and GLAST (*Slc1a3*), a glutamate transporter required for extracellular glutamate clearance and prevention of neuronal toxicity [112, 113]. Interestingly, GLAST is also reduced in *Dicer*-deficient postnatal astrocytes, in a $mGfap^{Cre}$:$Dicer^{fl/fl}$ mouse model, causing cerebellar degeneration [113]. Both *Nav2* and *Slc1a3* are not reduced in microglia isolated from mSOD1 mice, implying their reduction in $Cx3cr1^{\underline{Cre}}$:$Dicer^{fl/fl}$ microglia is not due to environmental tissue damage and resulting inflammatory conditions, but might be a direct result of *Dicer* deficiency. Accordingly, our adult microglia miR profile revealed high expression of specific miRs possibly important for microglia dependent neuronal circuits formation. MiR-181b has for instance been shown to induce MMP2 activity in cancer cell lines via targeting of its endogenous inhibitor TIMP3 [87]. Interestingly, MMP2 is involved in neuronal circuits formation by regulating neurogenesis, neuronal migration and axonal outgrowth [88, 89]. MiR-181b transcript levels are increased in embryonic microglia compared with adult microglia [21], suggesting its possible involvement in microglia function during embryogenesis. Interestingly, *Mmp2* expression is reduced in $Cx3cr1^{\underline{Cre}}$:$Dicer^{fl/fl}$ adult microglia, possibly reflecting an earlier prenatal reduction due to lack of miR-181b expression. It could be that absence of the above genes, although they are generally required for neuronal maintenance by microglia, are more detrimental in embryonic stages, and therefore a neuronal damage phenotype is observed in the $Cx3cr1^{\underline{Cre}}$:$Dicer^{fl/fl}$, but not $Cx3cr1^{\underline{CreER}}$:$Dicer^{fl/-}$ mice. We therefore suggest that miRs are essential for unique functions of embryonic microglia such as their support of neurogenesis, neuronal survival, and differentiation [17, 39, 137]. Accordingly, the microglial *Dicer* deficiency at embryonic stage might result in a substantial damage to the neuronal network in various areas of the brain and SC, including regions directly involved in hind limb motorics, such as the SC-L5 ventral horn, while the same deficiency in later postnatal stages does not lead to neuronal damage, as demonstrated in the $Cx3cr1^{\underline{CreER}}$:$Dicer^{fl/-}$ mice (**Scheme 7**). On the other hand, although gross motoric functions of $Cx3cr1^{\underline{CreER}}$:$Dicer^{fl/-}$ mice are intact, it could be that motor skill learning abilities required for motor improvement and are dependent on microglial synaptic pruning of the adult motor cortex [18] will require intact *Dicer* activity in

adult microglia.

In addition to their homeostatic function, adult microglia were shown to play a role in various neurodegenerative diseases, further exacerbating tissue damage by the secretion of pro-inflammatory and neurotoxic factors [50, 53, 60, 97]. MiRs were shown to have an anti-inflammatory effect on microglia activation [71, 76, 77] and to attenuate neurodegenerative diseases [70]. On the other hand, some miRs, such as miR-155 were suggested to contribute to disease severity in mSOD1 mice [73]. Therefore, it would be interesting to explore the activation threshold of adult *Cx3cr1*^{CreER}*:Dicer*$^{fl/-}$ microglia and test disease severity in challenged *Cx3cr1*^{CreER}*:Dicer*$^{fl/-}$ mice in the context of neurodegenerative processes. In order to reveal transcriptional changes occurring in postnatally targeted *Cx3cr1*^{CreER}*:Dicer*$^{fl/-}$ microglia, we intend to perform an mRNA sequencing analysis of these cells.

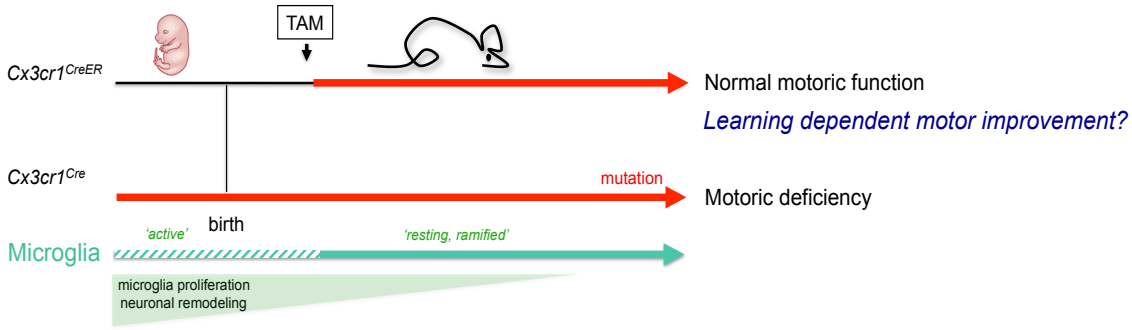

Figure 16. Comparison of the Cx3cr1^{Cre} vs. Cx3cr1^{CreER} Dicer deletion in Microglia.
A schematic timeline showing embryonic microglia *Dicer* deletion (red) in the non-inducible mouse model (*Cx3cr1*^{Cre}), compared with postnatal microglia *Dicer* deletion in the tamoxifen-inducible mouse model (*Cx3cr1*^{CreER}). Embryonic *Dicer* deletion results in a motoric deficiency, while postnatal *Dicer* deletion results in no obvious motoric impairment. Interestingly, microglia shift phenotype between these two life stages from activated highly proliferative to resting and ramified (see Figure 4).

Interestingly, microglia in both *Cx3cr1*^{Cre}*:Dicer*$^{fl/fl}$ and tamoxifen-treated *Cx3cr1*^{CreER}*:Dicer*$^{fl/-}$ mice models become radiosensitive, as demonstated by the fact that a BM engraftment following lethal irradiation results in their efficient replacement. This finding is in line with a recent report that Dicer is required for a proper DNA damage response to irradiation [115] albeit, this activity is independend of miRs but rather involves other non-coding RNAs that require processing by dicer. While *Cx3cr1*^{Cre}*:Dicer*$^{fl/fl}$ mice displayed a complete (>90%) substitution of microglia by BM-derived cells, *Cx3cr1*^{CreER}*:Dicer*$^{fl/-}$ mice showed a partial 40% substitution out of local microglia population. The remaining resident microglia constituted endogenous cells targeted by the tamoxifen treatment (as indicated by reporter gene

expression, YFP) that however retained the *Dicer* allele and can be considered "WT cells". This cells represent an initially rare population that only went through one recombination event, a technical imperfection of tamoxifen induced recombination, however in this particular case, WT cells will increase with time on the expense of Dicer deleted cells due to a survival advantage, as shown before [98]. Of note, the transfer experiment was performed 6 months post tamoxifen treatment, allowing for partial out-competition of the *Dicer*-deficient cells and probably earlier time points post tamoxifen treatment reflect Dicer deletion in the majority of microglia population.

In conclusion, our data support the emerging notion that microglia are pivotal players in the establishment and maintenance of neuronal networks, fulfilling distinct roles during development and adulthood. Embryonic, but not adult introduction of miR deficiency in microglia causes neuronal damage and motoric impairment. Further studies are required to uncover the direct molecular changes in *Dicer* deficient embryonic microglia. In addition, although no spontaneous overt phenotype in $Cx3cr1^{\underline{CreER}}$:$Dicer^{fl/-}$ mice was observed, the absence of Dicer likely impacts on the gene expression profile and the function of these cells. While our data show that adult microglial quiescence can be maintained for a prolonged period of time in absence of miRs, this important post-transcriptional regulatory circuit might well affect experienced learning via synaptic pruning. In addition, it remains to be tested how Dicer- deficient microglia perform during challenge and upon encounter of neuronal tissue damage in the context of a neurodegenerative disease.

5. Declaration

This thesis summarizes my independent research projects in the laboratory of Prof. Steffen Jung. I was responsible for the design, execution and analysis of all the results experiments described in this thesis together with my supervisor Prof. Steffen Jung. The histological analysis including the immunefluorescent staining and microscopic analysis of the Dicer-deficient microglia phenotype has been done in close collaboration with the group of Prof. Marco Printz from Universitats Klinikum, Freiburg Germany.

6. References.

1. Schulz, C., et al., *A lineage of myeloid cells independent of Myb and hematopoietic stem cells.* Science, 2012. **336**(6077): p. 86-90.
2. Gautier, E.L., et al., *Gene-expression profiles and transcriptional regulatory pathways that underlie the identity and diversity of mouse tissue macrophages.* Nature immunology, 2012. **13**(11): p. 1118-28.
3. Ginhoux, F., et al., *Origin and differentiation of microglia.* Front Cell Neurosci, 2013. **7**: p. 45.
4. Ginhoux, F., et al., *Fate Mapping Analysis Reveals That Adult Microglia Derive from Primitive Macrophages.* Science, 2010. **330**(6005): p. 841-845.
5. Ajami, B., et al., *Infiltrating monocytes trigger EAE progression, but do not contribute to the resident microglia pool.* Nat Neurosci, 2011. **14**(9): p. 1142-1149.
6. Shechter, R., et al., *Infiltrating blood-derived macrophages are vital cells playing an anti-inflammatory role in recovery from spinal cord injury in mice.* PLoS medicine, 2009. **6**(7): p. e1000113.
7. Davalos, D., et al., *ATP mediates rapid microglial response to local brain injury in vivo.* Nat Neurosci, 2005. **8**(6): p. 752-8.
8. Nimmerjahn, A., F. Kirchhoff, and F. Helmchen, *Resting microglial cells are highly dynamic surveillants of brain parenchyma in vivo.* Science, 2005. **308**(5726): p. 1314-8.
9. Paolicelli, R.C., et al., *Synaptic Pruning by Microglia Is Necessary for Normal Brain Development.* Science, 2011. **333**(6048): p. 1456-1458.
10. Schafer, D.P., et al., *Microglia sculpt postnatal neural circuits in an activity and complement-dependent manner.* Neuron, 2012. **74**(4): p. 691-705.
11. Stevens, B., et al., *The classical complement cascade mediates CNS synapse elimination.* Cell, 2007. **131**(6): p. 1164-78.
12. Chiu, I.M., et al., *A neurodegeneration-specific gene-expression signature of acutely isolated microglia from an amyotrophic lateral sclerosis mouse model.* Cell Rep, 2013. **4**(2): p. 385-401.
13. Butovsky, O., et al., *Identification of a unique TGF-beta-dependent molecular and functional signature in microglia.* Nat Neurosci, 2014. **17**(1): p. 131-43.
14. Ajami, B., et al., *Local self-renewal can sustain CNS microglia maintenance and function throughout adult life.* Nat Neurosci, 2007. **10**(12): p. 1538-43.
15. Marin-Teva, J.L., et al., *Microglia promote the death of developing Purkinje cells.* Neuron, 2004. **41**(4): p. 535-47.
16. Squarzoni, P., et al., *Microglia modulate wiring of the embryonic forebrain.* Cell Rep, 2014. **8**(5): p. 1271-9.
17. Ueno, M., et al., *Layer V cortical neurons require microglial support for survival during postnatal development.* Nat Neurosci, 2013. **16**(5): p. 543-51.
18. Parkhurst, C.N., et al., *Microglia promote learning-dependent synapse formation through brain-derived neurotrophic factor.* Cell, 2013. **155**(7): p. 1596-609.
19. Tremblay, M.E., R.L. Lowery, and A.K. Majewska, *Microglial interactions with synapses are modulated by visual experience.* PLoS Biol, 2010. **8**(11): p. e1000527.

20. Wake, H., et al., *Resting microglia directly monitor the functional state of synapses in vivo and determine the fate of ischemic terminals.* J Neurosci, 2009. **29**(13): p. 3974-80.
21. Kierdorf, K., et al., *Microglia emerge from erythromyeloid precursors via Pu.1- and Irf8-dependent pathways.* Nat Neurosci, 2013. **16**(3): p. 273-80.
22. Olah, M., et al., *Identification of a microglia phenotype supportive of remyelination.* Glia, 2012. **60**(2): p. 306-21.
23. Perry, V.H., D.A. Hume, and S. Gordon, *Immunohistochemical localization of macrophages and microglia in the adult and developing mouse brain.* Neuroscience, 1985. **15**(2): p. 313-26.
24. Schlegelmilch, T., K. Henke, and F. Peri, *Microglia in the developing brain: from immunity to behaviour.* Curr Opin Neurobiol, 2011. **21**(1): p. 5-10.
25. Swinnen, N., et al., *Complex invasion pattern of the cerebral cortex bymicroglial cells during development of the mouse embryo.* Glia, 2013. **61**(2): p. 150-63.
26. Verney, C., et al., *Early microglial colonization of the human forebrain and possible involvement in periventricular white-matter injury of preterm infants.* J Anat, 2010. **217**(4): p. 436-48.
27. Bessis, A., et al., *Microglial control of neuronal death and synaptic properties.* Glia, 2007. **55**(3): p. 233-8.
28. Wakselman, S., et al., *Developmental neuronal death in hippocampus requires the microglial CD11b integrin and DAP12 immunoreceptor.* J Neurosci, 2008. **28**(32): p. 8138-43.
29. Xavier, A.L., et al., *Fine-tuning the central nervous system: microglial modelling of cells and synapses.* Philos Trans R Soc Lond B Biol Sci, 2014. **369**(1654): p. 20130593.
30. Erblich, B., et al., *Absence of colony stimulation factor-1 receptor results in loss of microglia, disrupted brain development and olfactory deficits.* PLoS One, 2011. **6**(10): p. e26317.
31. Pont-Lezica, L., et al., *Physiological roles of microglia during development.* J Neurochem, 2011. **119**(5): p. 901-8.
32. Antony, J.M., et al., *Endogenous microglia regulate development of embryonic cortical precursor cells.* J Neurosci Res, 2011. **89**(3): p. 286-98.
33. Mallat, M., J.L. Marin-Teva, and C. Cheret, *Phagocytosis in the developing CNS: more than clearing the corpses.* Curr Opin Neurobiol, 2005. **15**(1): p. 101-7.
34. Ni, L., et al., *Toll-like receptor ligands and CD154 stimulate microglia to produce a factor(s) that promotes excess cholinergic differentiation in the developing rat basal forebrain: implications for neurodevelopmental disorders.* Pediatr Res, 2007. **61**(1): p. 15-20.
35. Aarum, J., et al., *Migration and differentiation of neural precursor cells can be directed by microglia.* Proc Natl Acad Sci U S A, 2003. **100**(26): p. 15983-8.
36. Jonakait, G.M., et al., *Macrophage cell-conditioned medium promotes cholinergic differentiation of undifferentiated progenitors and synergizes with nerve growth factor action in the developing basal forebrain.* Exp Neurol, 2000. **161**(1): p. 285-96.
37. Sierra, A., et al., *Microglia Shape Adult Hippocampal Neurogenesis through Apoptosis-Coupled Phagocytosis.* Cell stem cell, 2010. **7**(4): p. 483-495.

38. Tremblay, M.E., et al., *The role of microglia in the healthy brain.* The Journal of neuroscience : the official journal of the Society for Neuroscience, 2011. **31**(45): p. 16064-9.
39. Harry, G.J., *Microglia during development and aging.* Pharmacol Ther, 2013. **139**(3): p. 313-26.
40. Imamoto, K. and C.P. Leblond, *Radioautographic investigation of gliogenesis in the corpus callosum of young rats. II. Origin of microglial cells.* J Comp Neurol, 1978. **180**(1): p. 139-63.
41. Orlowski, D., Z. Soltys, and K. Janeczko, *Morphological development of microglia in the postnatal rat brain. A quantitative study.* Int J Dev Neurosci, 2003. **21**(8): p. 445-50.
42. Zusso, M., et al., *Regulation of postnatal forebrain amoeboid microglial cell proliferation and development by the transcription factor Runx1.* J Neurosci, 2012. **32**(33): p. 11285-98.
43. Linnartz, B. and H. Neumann, *Microglial activatory (immunoreceptor tyrosine-based activation motif)- and inhibitory (immunoreceptor tyrosine-based inhibition motif)-signaling receptors for recognition of the neuronal glycocalyx.* Glia, 2013. **61**(1): p. 37-46.
44. Frank-Cannon, T.C., et al., *Does neuroinflammation fan the flame in neurodegenerative diseases?* Mol Neurodegener, 2009. **4**: p. 47.
45. Prinz, M. and A. Mildner, *Microglia in the CNS: Immigrants from another world.* Glia, 2011. **59**(2): p. 177-187.
46. Falsig, J., et al., *Molecular basis for detection of invading pathogens in the brain.* J Neurosci Res, 2008. **86**(7): p. 1434-47.
47. Saijo, K. and C.K. Glass, *Microglial cell origin and phenotypes in health and disease.* Nat Rev Immunol, 2011. **11**(11): p. 775-87.
48. Gurney, M.E., *Transgenic-mouse model of amyotrophic lateral sclerosis.* N Engl J Med, 1994. **331**(25): p. 1721-2.
49. Beers, D.R., et al., *Wild-type microglia extend survival in PU.1 knockout mice with familial amyotrophic lateral sclerosis.* Proc Natl Acad Sci U S A, 2006. **103**(43): p. 16021-6.
50. Frakes, A.E., et al., *Microglia induce motor neuron death via the classical NF-kappaB pathway in amyotrophic lateral sclerosis.* Neuron, 2014. **81**(5): p. 1009-23.
51. Goverman, J., *Autoimmune T cell responses in the central nervous system.* Nat Rev Immunol, 2009. **9**(6): p. 393-407.
52. Ponomarev, E.D., et al., *Microglial cell activation and proliferation precedes the onset of CNS autoimmunity.* J Neurosci Res, 2005. **81**(3): p. 374-89.
53. Goldmann, T. and M. Prinz, *Role of microglia in CNS autoimmunity.* Clin Dev Immunol, 2013. **2013**: p. 208093.
54. Guo, H., et al., *Mammalian microRNAs predominantly act to decrease target mRNA levels.* Nature, 2010. **466**(7308): p. 835-40.
55. Kosik, K.S., *The neuronal microRNA system.* Nat Rev Neurosci, 2006. **7**(12): p. 911-20.
56. Shi, Y., et al., *MicroRNA regulation of neural stem cells and neurogenesis.* J Neurosci, 2010. **30**(45): p. 14931-6.
57. Zhao, X., et al., *MicroRNA-mediated control of oligodendrocyte differentiation.* Neuron, 2010. **65**(5): p. 612-26.

58. Butovsky, O., et al., *Modulating inflammatory monocytes with a unique microRNA gene signature ameliorates murine ALS.* J Clin Invest, 2012. **122**(9): p. 3063-87.
59. Haramati, S., et al., *miRNA malfunction causes spinal motor neuron disease.* Proc Natl Acad Sci U S A, 2010. **107**(29): p. 13111-6.
60. Ponomarev, E.D., T. Veremeyko, and H.L. Weiner, *MicroRNAs are universal regulators of differentiation, activation, and polarization of microglia and macrophages in normal and diseased CNS.* Glia, 2013. **61**(1): p. 91-103.
61. Bartel, D.P., *MicroRNAs: target recognition and regulatory functions.* Cell, 2009. **136**(2): p. 215-33.
62. Asirvatham, A.J., et al., *MicroRNA targets in immune genes and the Dicer/Argonaute and ARE machinery components.* Mol Immunol, 2008. **45**(7): p. 1995-2006.
63. Lal, A., et al., *miR-24 Inhibits cell proliferation by targeting E2F2, MYC, and other cell-cycle genes via binding to "seedless" 3'UTR microRNA recognition elements.* Mol Cell, 2009. **35**(5): p. 610-25.
64. Tay, Y., et al., *MicroRNAs to Nanog, Oct4 and Sox2 coding regions modulate embryonic stem cell differentiation.* Nature, 2008. **455**(7216): p. 1124-8.
65. Schwartz, J.C., et al., *Antisense transcripts are targets for activating small RNAs.* Nat Struct Mol Biol, 2008. **15**(8): p. 842-8.
66. Vasudevan, S., Y. Tong, and J.A. Steitz, *Switching from repression to activation: microRNAs can up-regulate translation.* Science, 2007. **318**(5858): p. 1931-4.
67. Barca-Mayo, O. and Q.R. Lu, *Fine-Tuning Oligodendrocyte Development by microRNAs.* Front Neurosci, 2012. **6**: p. 13.
68. Kim, J., et al., *A MicroRNA feedback circuit in midbrain dopamine neurons.* Science, 2007. **317**(5842): p. 1220-4.
69. Junn, E. and M.M. Mouradian, *MicroRNAs in neurodegenerative diseases and their therapeutic potential.* Pharmacol Ther, 2012. **133**(2): p. 142-50.
70. Ponomarev, E.D., et al., *MicroRNA-124 promotes microglia quiescence and suppresses EAE by deactivating macrophages via the C/EBP-[alpha]-PU.1 pathway.* Nat Med, 2010. **advance online publication**.
71. Guedes, J., A.L. Cardoso, and M.C. Pedroso de Lima, *Involvement of microRNA in microglia-mediated immune response.* Clin Dev Immunol, 2013. **2013**: p. 186872.
72. Cardoso, A.L., et al., *miR-155 modulates microglia-mediated immune response by down-regulating SOCS-1 and promoting cytokine and nitric oxide production.* Immunology, 2012. **135**(1): p. 73-88.
73. Butovsky, O., et al., *Targeting miR-155 restores abnormal microglia and attenuates disease in SOD1 mice.* Ann Neurol, 2014.
74. Taganov, K.D., et al., *NF-kappaB-dependent induction of microRNA miR-146, an inhibitor targeted to signaling proteins of innate immune responses.* Proc Natl Acad Sci U S A, 2006. **103**(33): p. 12481-6.
75. Saba, R., et al., *MicroRNA 146a (miR-146a) is over-expressed during prion disease and modulates the innate immune response and the microglial activation state.* PLoS One, 2012. **7**(2): p. e30832.
76. Zhang, L., et al., *miR-21 represses FasL in microglia and protects against microglia-mediated neuronal cell death following hypoxia/ischemia.* Glia, 2012. **60**(12): p. 1888-95.

77. Zhang, L., et al., *The microRNA miR-181c controls microglia-mediated neuronal apoptosis by suppressing tumor necrosis factor.* J Neuroinflammation, 2012. **9**: p. 211.
78. Beutner, C., et al., *Unique transcriptome signature of mouse microglia.* Glia, 2013. **61**(9): p. 1429-42.
79. Wolf, Y., et al., *Microglia, seen from the CX3CR1 angle.* Frontiers in Cellular Neuroscience, 2013. **7**.
80. Yona, S., et al., *Fate Mapping Reveals Origins and Dynamics of Monocytes and Tissue Macrophages under Homeostasis.* Immunity, 2013. **38**(1): p. 79-91.
81. Jung, S., et al., *Analysis of fractalkine receptor CX(3)CR1 function by targeted deletion and green fluorescent protein reporter gene insertion.* Mol Cell Biol, 2000. **20**(11): p. 4106-14.
82. Feil, S., N. Valtcheva, and R. Feil, *Inducible Cre mice.* Methods Mol Biol, 2009. **530**: p. 343-63.
83. Ach, R.A., H. Wang, and B. Curry, *Measuring microRNAs: comparisons of microarray and quantitative PCR measurements, and of different total RNA prep methods.* BMC Biotechnol, 2008. **8**: p. 69.
84. Muley, P.D., et al., *The atRA-responsive gene neuron navigator 2 functions in neurite outgrowth and axonal elongation.* Dev Neurobiol, 2008. **68**(13): p. 1441-53.
85. Harrison, S.J., et al., *Sall1 regulates cortical neurogenesis and laminar fate specification in mice: implications for neural abnormalities in Townes-Brocks syndrome.* Dis Model Mech, 2012. **5**(3): p. 351-65.
86. Qin, L., et al., *NADPH oxidase and aging drive microglial activation, oxidative stress, and dopaminergic neurodegeneration following systemic LPS administration.* Glia, 2013. **61**(6): p. 855-68.
87. Wang, B., et al., *TGFbeta-mediated upregulation of hepatic miR-181b promotes hepatocarcinogenesis by targeting TIMP3.* Oncogene, 2010. **29**(12): p. 1787-97.
88. Saygili, E., et al., *Sympathetic neurons express and secrete MMP-2 and MT1-MMP to control nerve sprouting via pro-NGF conversion.* Cell Mol Neurobiol, 2011. **31**(1): p. 17-25.
89. Vaillant, C., et al., *Spatiotemporal expression patterns of metalloproteinases and their inhibitors in the postnatal developing rat cerebellum.* J Neurosci, 1999. **19**(12): p. 4994-5004.
90. Harfe, B.D., et al., *The RNaseIII enzyme Dicer is required for morphogenesis but not patterning of the vertebrate limb.* Proc Natl Acad Sci U S A, 2005. **102**(31): p. 10898-903.
91. Rusca, N. and S. Monticelli, *MiR-146a in Immunity and Disease.* Mol Biol Int, 2011. **2011**: p. 437301.
92. Barbeito, L.H., et al., *A role for astrocytes in motor neuron loss in amyotrophic lateral sclerosis.* Brain Res Brain Res Rev, 2004. **47**(1-3): p. 263-74.
93. Chiu, I.M., et al., *Activation of innate and humoral immunity in the peripheral nervous system of ALS transgenic mice.* Proc Natl Acad Sci U S A, 2009. **106**(49): p. 20960-5.
94. Fischer, L.R., et al., *Amyotrophic lateral sclerosis is a distal axonopathy: evidence in mice and man.* Exp Neurol, 2004. **185**(2): p. 232-40.

95. Rotshenker, S., *Wallerian degeneration: the innate-immune response to traumatic nerve injury.* J Neuroinflammation, 2011. **8**: p. 109.
96. Reichert, F., A. Saada, and S. Rotshenker, *Peripheral nerve injury induces Schwann cells to express two macrophage phenotypes: phagocytosis and the galactose-specific lectin MAC-2.* J Neurosci, 1994. **14**(5 Pt 2): p. 3231-45.
97. Block, M.L., L. Zecca, and J.S. Hong, *Microglia-mediated neurotoxicity: uncovering the molecular mechanisms.* Nat Rev Neurosci, 2007. **8**(1): p. 57-69.
98. Kuipers, H., et al., *Dicer-dependent microRNAs control maturation, function, and maintenance of Langerhans cells in vivo.* J Immunol, 2010. **185**(1): p. 400-9.
99. de Haas, A.H., H.W. Boddeke, and K. Biber, *Region-specific expression of immunoregulatory proteins on microglia in the healthy CNS.* Glia, 2008. **56**(8): p. 888-94.
100. Park, L., et al., *Nox2-derived radicals contribute to neurovascular and behavioral dysfunction in mice overexpressing the amyloid precursor protein.* Proc Natl Acad Sci U S A, 2008. **105**(4): p. 1347-52.
101. Bouchon, A., et al., *TREM-1 amplifies inflammation and is a crucial mediator of septic shock.* Nature, 2001. **410**(6832): p. 1103-7.
102. Ehrchen, J.M., et al., *The endogenous Toll-like receptor 4 agonist S100A8/S100A9 (calprotectin) as innate amplifier of infection, autoimmunity, and cancer.* J Leukoc Biol, 2009. **86**(3): p. 557-66.
103. Postler, E., et al., *Expression of the S-100 proteins MRP-8 and -14 in ischemic brain lesions.* Glia, 1997. **19**(1): p. 27-34.
104. Shepherd, C.E., et al., *Inflammatory S100A9 and S100A12 proteins in Alzheimer's disease.* Neurobiol Aging, 2006. **27**(11): p. 1554-63.
105. Flo, T.H., et al., *Lipocalin 2 mediates an innate immune response to bacterial infection by sequestrating iron.* Nature, 2004. **432**(7019): p. 917-21.
106. Bi, F., et al., *Reactive astrocytes secrete lcn2 to promote neuron death.* Proc Natl Acad Sci U S A, 2013. **110**(10): p. 4069-74.
107. Jang, E., et al., *Secreted protein lipocalin-2 promotes microglial M1 polarization.* FASEB J, 2013. **27**(3): p. 1176-90.
108. Lee, S., et al., *A dual role of lipocalin 2 in the apoptosis and deramification of activated microglia.* J Immunol, 2007. **179**(5): p. 3231-41.
109. Chabas, D., et al., *The influence of the proinflammatory cytokine, osteopontin, on autoimmune demyelinating disease.* Science, 2001. **294**(5547): p. 1731-5.
110. Hashimoto, M., et al., *Osteopontin-deficient mice exhibit less inflammation, greater tissue damage, and impaired locomotor recovery from spinal cord injury compared with wild-type controls.* J Neurosci, 2007. **27**(13): p. 3603-11.
111. McNeill, E.M., et al., *Nav2 is necessary for cranial nerve development and blood pressure regulation.* Neural Dev, 2010. **5**: p. 6.
112. Sheldon, A.L. and M.B. Robinson, *The role of glutamate transporters in neurodegenerative diseases and potential opportunities for intervention.* Neurochem Int, 2007. **51**(6-7): p. 333-55.
113. Tao, J., et al., *Deletion of astroglial Dicer causes non-cell-autonomous neuronal dysfunction and degeneration.* J Neurosci, 2011. **31**(22): p. 8306-19.

114. Derecki, N.C., et al., *Wild-type microglia arrest pathology in a mouse model of Rett syndrome.* Nature, 2012. **484**(7392): p. 105-9.
115. Francia, S., et al., *Site-specific DICER and DROSHA RNA products control the DNA-damage response.* Nature, 2012. **488**(7410): p. 231-5.
116. Chorro, L. and F. Geissmann, *Development and homeostasis of 'resident' myeloid cells: the case of the Langerhans cell.* Trends Immunol, 2010. **31**(12): p. 438-45.
117. Chorro, L., et al., *Langerhans cell (LC) proliferation mediates neonatal development, homeostasis, and inflammation-associated expansion of the epidermal LC network.* J Exp Med, 2009. **206**(13): p. 3089-100.
118. Bain, C.C., et al., *Constant replenishment from circulating monocytes maintains the macrophage pool in the intestine of adult mice.* Nat Immunol, 2014. **15**(10): p. 929-37.
119. Goldmann, T., et al., *A new type of microglia gene targeting shows TAK1 to be pivotal in CNS autoimmune inflammation.* Nat Neurosci, 2013. **16**(11): p. 1618-26.
120. Bernstein, E., et al., *Dicer is essential for mouse development.* Nat Genet, 2003. **35**(3): p. 215-7.
121. Lallemand, Y., et al., *Maternally expressed PGK-Cre transgene as a tool for early and uniform activation of the Cre site-specific recombinase.* Transgenic Res, 1998. **7**(2): p. 105-12.
122. Srinivas, S., et al., *Cre reporter strains produced by targeted insertion of EYFP and ECFP into the ROSA26 locus.* BMC developmental biology, 2001. **1**: p. 4.
123. Zigmond, E., et al., *Ly6C hi monocytes in the inflamed colon give rise to proinflammatory effector cells and migratory antigen-presenting cells.* Immunity, 2012. **37**(6): p. 1076-90.
124. Zigmond, E., et al., *Infiltrating monocyte-derived macrophages and resident kupffer cells display different ontogeny and functions in acute liver injury.* J Immunol, 2014. **193**(1): p. 344-53.
125. Lewis, B.P., et al., *Prediction of mammalian microRNA targets.* Cell, 2003. **115**(7): p. 787-98.
126. Garber, M., et al., *A high-throughput chromatin immunoprecipitation approach reveals principles of dynamic gene regulation in mammals.* Mol Cell, 2012. **47**(5): p. 810-22.
127. Ransohoff, R.M. and V.H. Perry, *Microglial physiology: unique stimuli, specialized responses.* Annu Rev Immunol, 2009. **27**: p. 119-45.
128. Ouyang, Y.B., et al., *The Use of microRNAs to Modulate Redox and Immune Response to Stroke.* Antioxid Redox Signal, 2014.
129. Schaefer, A., et al., *Cerebellar neurodegeneration in the absence of microRNAs.* J Exp Med, 2007. **204**(7): p. 1553-8.
130. Hirata, K. and M. Kawabuchi, *Myelin phagocytosis by macrophages and nonmacrophages during Wallerian degeneration.* Microsc Res Tech, 2002. **57**(6): p. 541-7.
131. Wu, D.C., et al., *NADPH oxidase mediates oxidative stress in the 1-methyl-4-phenyl-1,2,3,6-tetrahydropyridine model of Parkinson's disease.* Proc Natl Acad Sci U S A, 2003. **100**(10): p. 6145-50.
132. Jekabsone, A., et al., *Fibrillar beta-amyloid peptide Abeta1-40 activates microglial proliferation via stimulating TNF-alpha release and H2O2 derived*

from NADPH oxidase: a cell culture study. J Neuroinflammation, 2006. **3**: p. 24.
133. Qin, B., et al., *A key role for the microglial NADPH oxidase in APP-dependent killing of neurons.* Neurobiol Aging, 2006. **27**(11): p. 1577-87.
134. Akiyama, H., et al., *Expression of MRP14, 27E10, interferon-alpha and leukocyte common antigen by reactive microglia in postmortem human brain tissue.* J Neuroimmunol, 1994. **50**(2): p. 195-201.
135. Verbeek, M.M., et al., *A lysosomal marker for activated microglial cells involved in Alzheimer classic senile plaques.* Acta Neuropathol, 1995. **90**(5): p. 493-503.
136. Comi, C., et al., *Osteopontin is increased in the cerebrospinal fluid of patients with Alzheimer's disease and its levels correlate with cognitive decline.* J Alzheimers Dis, 2010. **19**(4): p. 1143-8.
137. Ueno, M. and T. Yamashita, *Bidirectional tuning of microglia in the developing brain: from neurogenesis to neural circuit formation.* Curr Opin Neurobiol, 2014. **27**: p. 8-15.